

TENSOR PRODUCTS OF A_∞ -ALGEBRAS WITH HOMOTOPY INNER PRODUCTS

THOMAS TRADLER¹ AND RONALD UMBLE²

ABSTRACT. We show that the tensor product of two cyclic A_∞ -algebras is, in general, not a cyclic A_∞ -algebra, but an A_∞ -algebra with homotopy inner product. More precisely, following Markl and Shnider in [MS], we construct an explicit combinatorial diagonal on the pairahedra, which are contractible polytopes controlling the combinatorial structure of an A_∞ -algebra with homotopy inner products, and use it to define a categorically closed tensor product. A cyclic A_∞ -algebra can be thought of as an A_∞ -algebra with homotopy inner products whose higher inner products are trivial. However, the higher inner products on the tensor product of cyclic A_∞ -algebras are not necessarily trivial.

1. INTRODUCTION

Let R be a commutative ring with unity and let $C_*(K)$ denote the cellular chains of associahedra $K = \sqcup_{n \geq 2} K_n$, see [S]. Identify $C_*(K)$ with the A_∞ -operad \mathcal{A}_∞ and consider the Sanedidze-Umble (S-U) diagonal $\Delta_K : C_*(K) \rightarrow C_*(K) \otimes C_*(K)$ [SU]. Given A_∞ -algebras $(A, \mu_n)_{n \geq 1}$ and $(B, \nu_n)_{n \geq 1}$ over R , represent A and B as algebras over \mathcal{A}_∞ via operadic maps $\{\zeta_A : C_*(K_n) \rightarrow \text{Hom}(A^{\otimes n}, A)\}_{n \geq 1}$ and $\{\zeta_B : C_*(K_n) \rightarrow \text{Hom}(B^{\otimes n}, B)\}_{n \geq 1}$. Define $\varphi_1 = \mu_1 \otimes \mathbf{1} + \mathbf{1} \otimes \nu_1$ and

$$\varphi_n = [(\zeta_A \otimes \zeta_B) \Delta_K (e^{n-2})] \sigma_n,$$

where $\sigma_n : (A \otimes B)^{\otimes n} \rightarrow A^{\otimes n} \otimes B^{\otimes n}$ is the canonical permutation of tensor factors and e^{n-2} denotes the top dimensional cell of K_n . Then $(A \otimes B, \varphi_n)_{n \geq 1}$ is an A_∞ -algebra, and for example,

$$\varphi_2 = (\mu_2 \otimes \nu_2) \sigma_2 \quad \text{and} \quad \varphi_3 = [\mu_2(\mu_2 \otimes \mathbf{1}) \otimes \nu_3 + \mu_3 \otimes \nu_2(\mathbf{1} \otimes \nu_2)] \sigma_3.$$

An A_∞ -algebra (V, ρ_n) is *cyclic* if V is equipped with a cyclically invariant inner product $\langle -, - \rangle_V$, i.e., $\langle \rho_n(a_1, \dots, a_n), a_{n+1} \rangle_V = (-1)^\epsilon \langle \rho_n(a_2, \dots, a_{n+1}), a_1 \rangle_V$. Thus if (A, μ_n) and (B, ν_n) are cyclic, it is natural to ask whether $\langle -, - \rangle_A$ and $\langle -, - \rangle_B$ induce a cyclically invariant inner product on $(A \otimes B, \varphi_n)$. As a first approximation, consider the inner product

$$\langle a_1|b_1, a_2|b_2 \rangle_{A \otimes B} = (-1)^{|a_2||b_1|} \langle a_1, a_2 \rangle_A \langle b_1, b_2 \rangle_B,$$

which respects φ_1 and φ_2 but not φ_3 since

$$\langle \varphi_3(a_1|b_1, a_2|b_2, a_3|b_3), a_4|b_4 \rangle - (-1)^\epsilon \langle \varphi_3(a_2|b_2, a_3|b_3, a_4|b_4), a_1|b_1 \rangle \neq 0.$$

Date: submitted August 25, 2011; revised February 9, 2012.

2010 Mathematics Subject Classification. 55S15, 52B05, 18D50, 55U99.

Key words and phrases. A_∞ -algebra with homotopy inner product, colored operad, cyclic A_∞ -algebra, diagonal, pairahedron, tensor product, W-construction.

¹ This research funded in part by the PSC-CUNY grant PSCREG-41-316.

² This research funded in part by a Millersville University faculty research grant.

However, there is a chain homotopy $\varrho_{2,0} : (A \otimes B)^{\otimes 4} \rightarrow R$ such that

$$\begin{aligned} (\varrho_{2,0} \circ d)(a_1|b_1, a_2|b_2, a_3|b_3, a_4|b_4) = \\ \langle \varphi_3(a_1|b_1, a_2|b_2, a_3|b_3), a_4|b_4 \rangle - (-1)^\epsilon \langle \varphi_3(a_2|b_2, a_3|b_3, a_4|b_4), a_1|b_1 \rangle, \end{aligned}$$

where d is the linear extension of φ_1 and

$$\varrho_{2,0}(x_1|y_1, x_2|y_2, x_3|y_3, x_4|y_4) = \pm \langle \mu_3(x_1, x_2, x_3), x_4 \rangle_A \langle y_1, \nu_3(y_2, y_3, y_4) \rangle_B.$$

Thus $\langle -, - \rangle_{A \otimes B}$ respects φ_3 up to a homotopy, and there is hope.

In [T1], the first author defined the notion of an A_∞ -algebra with homotopy inner product, which is an A_∞ -algebra (A, μ_n) together with “compatible” families of module maps

$$\{\lambda_{j,k} : A^{\otimes j} \otimes A \otimes A^{\otimes k} \rightarrow A\}_{j,k \geq 0}$$

and higher inner products

$$\{\varrho_{j,k} : A \otimes A^{\otimes j} \otimes A \otimes A^{\otimes k} \rightarrow R\}_{j,k \geq 0}.$$

Homotopy inner products appear in actions on moduli spaces (*e.g.* [T2, TZ]), in the deformation theory of inner products [TT], and in symplectic structures on formal non-commutative supermanifolds [C].

Following the construction of Markl and Shnider in [MS], we extend the inner product $\langle -, - \rangle_{A \otimes B}$ defined above to a homotopy inner product on $(A \otimes B, \varphi_n)$ as follows:

- (1) We identify the cellular chains of the associahedra and pairahedra with a three-colored operad $C_*\hat{\mathcal{A}}$ (the pairahedra, constructed by the first author in [T1], encode the relations among A_∞ -operations, module maps, and homotopy inner products).
- (2) We adapt Boardman and Vogt’s W -construction [BV] to obtain the three-colored operad $Q_*\hat{\mathcal{A}}$, which is a cubical decomposition of $C_*\hat{\mathcal{A}}$.
- (3) We define a quasi-invertible subdivision map $q : C_*\hat{\mathcal{A}} \rightarrow Q_*\hat{\mathcal{A}}$ whose quasi-inverse $p : Q_*\hat{\mathcal{A}} \rightarrow C_*\hat{\mathcal{A}}$ is defined in terms of an appropriate partial ordering on binary planar diagrams.
- (4) The Serre diagonal on cellular chains of the n -cube induces a coassociative diagonal $\Delta_Q : Q_*\hat{\mathcal{A}} \rightarrow Q_*\hat{\mathcal{A}} \otimes Q_*\hat{\mathcal{A}}$, which in turn induces a non-coassociative diagonal

$$\Delta_C : C_*\hat{\mathcal{A}} \xrightarrow{q} Q_*\hat{\mathcal{A}} \xrightarrow{\Delta_Q} Q_*\hat{\mathcal{A}} \otimes Q_*\hat{\mathcal{A}} \xrightarrow{p \otimes p} C_*\hat{\mathcal{A}} \otimes C_*\hat{\mathcal{A}}.$$

- (5) We represent the homotopy inner products on A and B as operadic maps $\psi_A : C_*\hat{\mathcal{A}} \rightarrow \mathcal{E}nd_A$ and $\psi_B : C_*\hat{\mathcal{A}} \rightarrow \mathcal{E}nd_B$, and define

$$\psi_{A \otimes B} : C_*\hat{\mathcal{A}} \xrightarrow{\Delta_C} C_*\hat{\mathcal{A}} \otimes C_*\hat{\mathcal{A}} \xrightarrow{\psi_A \otimes \psi_B} \mathcal{E}nd_A \otimes \mathcal{E}nd_B \xrightarrow{\cong} \mathcal{E}nd_{A \otimes B}.$$

The paper is organized as follows. Section 2 defines the three-colored operads $C_*\hat{\mathcal{A}}$ and $Q_*\hat{\mathcal{A}}$. The map $q : C_*\hat{\mathcal{A}} \rightarrow Q_*\hat{\mathcal{A}}$ is defined in Section 3 and a quasi-inverse p is defined in Section 4. Section 5 introduces the diagonal Δ_C , and we conclude the paper with some computations in Section 6. To maximize accessibility, longer proofs and other technical considerations are collected in the appendices. Signs are discussed in Appendix A; the contractibility of pairahedra is proved in Appendix B; the fact that relation “ \leq ” in the definition of the morphism p is a partial ordering is

established in Appendix C; and the fact that p is a chain map is proved in Appendix D.

2. THE THREE-COLORED OPERADS $C_*\hat{\mathcal{A}}$ AND $Q_*\hat{\mathcal{A}}$

In this section we construct the three-colored operads $C_*\hat{\mathcal{A}}$ and $Q_*\hat{\mathcal{A}}$. Algebras over $C_*\hat{\mathcal{A}}$ are A_∞ -algebras with homotopy inner products and $Q_*\hat{\mathcal{A}}$ is a cubical subdivision of $C_*\hat{\mathcal{A}}$. Both operads are defined in terms of three types of planar diagrams: (1) *planar trees*, which encode the homotopy associativity structure, (2) *module trees*, which encode the homotopy bimodule structure, and (3) *inner product diagrams*, which encode the homotopy inner product structure. We shall refer to a diagram in any of these categories as a *planar diagram*. The term *leaf* of a planar diagram will always refer to an external inward directed edge; the term *root* will always refer to the single external outward directed edge of a tree; and the term *edge* will always refer to an internal edge, which is neither a root nor a leaf.

Planar diagrams are generated by three families of corollas: $\{T_n\}_{n \geq 2}$, $\{M_{j,k}\}_{j+k \geq 0}$, and $\{I_{j,k}\}_{j+k \geq 0}$. The root and leaves of a corolla have one of three colors: *thick*, *thin*, or *empty*. The corolla T_n has n thin leaves and a thin root; $M_{j,k}$ has a thick vertical root, a thick vertical leaf, j thin leaves in the left half-plane, and k thin leaves in the right half-plane; and $I_{j,k}$ has an empty root, which is graphically represented by a thick vertex, two thick horizontal leaves, j thin leaves in the upper half-plane, and k thin leaves in the lower half-plane, all meeting at the thick vertex. An example of each type appears in Figure 1.

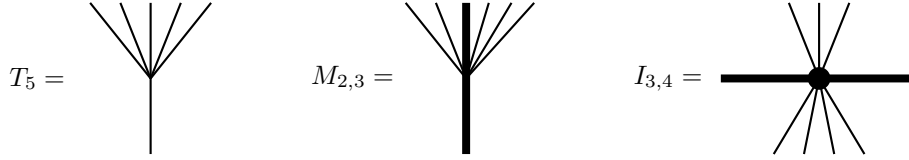


FIGURE 1. Three types of corollas

A planar tree T is composed with a diagram D by attaching the root of T to a thin leaf of D . Two module trees are composed by attaching the thick root of one to the thick leaf of the other. A module tree M is composed with an inner product diagram I by attaching the thick root of M to a thick leaf of I . Two inner product diagrams cannot be composed. A planar diagram resulting from each of the various compositions appears in Figure 2.

Given a planar diagram D , let $\mathcal{L}(D)$ denote the set of leaves of D . If $k = \#\mathcal{L}(D)$, we use a bijection $f : \{1, \dots, k\} \rightarrow \mathcal{L}(D)$ to label the elements of $\mathcal{L}(D)$. In particular, f_\circlearrowleft will denote the “canonical” labeling bijection, which numbers the leaves of a (planar or module) tree sequentially from left-to-right and the leaves of an inner product diagram clockwise starting with the left thick leaf (see Figure 3). Let $\mathcal{E}(D)$ denote the set of edges of a planar diagram D .

Definition 2.1. Define the **orientation** of a corolla to be $+1$ or -1 ; an **orientation** of a planar diagram D with $\mathcal{E}(D) = \{e_1, \dots, e_k\}$ is a formal skew-commutative product $\omega = e_{i_1} \wedge \dots \wedge e_{i_k}$. Thus D admits exactly two orientations: ω and $-\omega$.

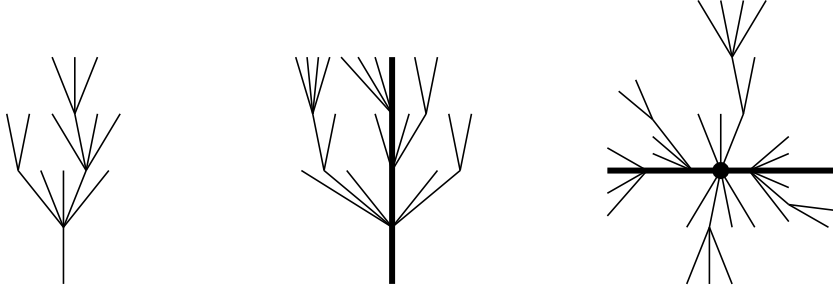


FIGURE 2. Three types of planar diagrams (a tree diagram T , a module diagram M , an inner product diagram I)

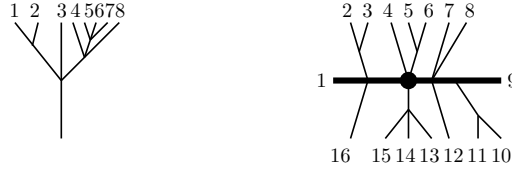


FIGURE 3. Canonical numbering f_{\circ} of the leaves of a diagram

Following the construction of the colored operad governing homotopy inner products in [LT], we define the three-colored operad $C_*\hat{\mathcal{A}}$. Let $\mathbb{Z}_3 = \{0, 1, 2\}$, and denote the empty color by 0, the thin color by 1, and the thick color by 2.

Definition 2.2. The **three-colored operad**

$$C_*\hat{\mathcal{A}} = \bigoplus_{\substack{\mathbf{x} \times \mathbf{y} \in \mathbb{Z}_3^{n+1} \\ n \geq 1}} C_*\hat{\mathcal{A}}_{\mathbf{y}}^{\mathbf{x}},$$

is the graded R -module in which $C_*\hat{\mathcal{A}}_{\mathbf{y}}^{\mathbf{x}} = 0$ unless

(i) $\mathbf{x} \times \mathbf{y} = 1 \cdots 1 \times 1 \in \mathbb{Z}_3^{n+1}$:

$C_*\hat{\mathcal{A}}_{\mathbf{y}}^{\mathbf{x}}$ is generated by triples (T, f, ω) modulo $(T, f, -\omega) = -(T, f, \omega)$, where T is a planar tree with n leaves and ω is an orientation on T .

(ii) $\mathbf{x} \times \mathbf{y} = 1 \cdots 121 \cdots 1 \times 2 \in \mathbb{Z}_3^{n+1}$ with 2 in the i^{th} position of \mathbf{x} :

$C_*\hat{\mathcal{A}}_{\mathbf{y}}^{\mathbf{x}}$ is generated by triples (M, f, ω) modulo $(M, f, -\omega) = -(M, f, \omega)$, where M is a module tree with n leaves of which $f(i)$ is thick, and ω is an orientation on M .

(iii) $\mathbf{x} \times \mathbf{y} = 1 \cdots 121 \cdots 121 \cdots 1 \times 0 \in \mathbb{Z}_3^{n+1}$ with 2 in the i^{th} and j^{th} positions:

$C_*\hat{\mathcal{A}}_{\mathbf{y}}^{\mathbf{x}}$ is generated by triples (I, f, ω) modulo $(I, f, -\omega) = -(I, f, \omega)$, where I is an inner product diagram with n leaves of which $f(i)$ and $f(j)$ are thick, and ω is an orientation on I .

The **coloring** of a generator $(D, f, \omega) \in C_*\hat{\mathcal{A}}_{\mathbf{y}}^{\mathbf{x}}$ is the pair $\mathbf{x} \times \mathbf{y}$, and its **degree**

$$|(D, f, \omega)| := \#\mathcal{L}(D) - \#\mathcal{E}(D) - 2.$$

When $|(D, f, \omega)| = n$, we write $(D, f, \omega) \in C_n \hat{\mathcal{A}}$. Formally adjoin **units** to $C_* \hat{\mathcal{A}}$ and define their degrees to be 0. Given an edge $e \in \mathcal{E}(D)$, let D/e denote the planar diagram obtained from D by contracting e to a point. Define the **boundary** of (D, f, ω) by

$$\partial_C(D, f, \omega) := \sum_{\substack{D'/e'=D \\ e' \in \mathcal{E}(D')}} (D', f, e' \wedge \omega),$$

summed over all diagrams D' and all edges $e' \in \mathcal{E}(D')$ such that $D'/e' = D$. The relation $\partial_C^2 = 0$ follows from the fact that $e' \wedge e'' \wedge \omega = -e'' \wedge e' \wedge \omega$. If $n = \#\mathcal{L}(D)$ and $\sigma \in S_n$, define the S_n -**action** by

$$\sigma \cdot (D, f, \omega) := \text{sgn}(\sigma) \cdot (D, f \circ \sigma, \omega).$$

Now, given generators $(D, f_D, \omega_D) \in C_m \hat{\mathcal{A}}$ and $(E, f_E, \omega_E) \in C_n \hat{\mathcal{A}}$, let $k = \#\mathcal{L}(D)$ and $l = \#\mathcal{L}(E)$. For $1 \leq i \leq k$, define the i^{th} **operadic composition** $(D, f_D, \omega_D) \circ_i (E, f_E, \omega_E)$ to be zero unless the root of E and the i^{th} input of D have the same color, in which case,

$$(2.1) \quad (D, f_D, \omega_D) \circ_i (E, f_E, \omega_E) := (-1)^\epsilon (D \circ_{f_D(i)} E, f_{D \circ E}, \omega_D \wedge \omega_E \wedge e),$$

where $\epsilon = i(l+1) + kn$, $D \circ_{f_D(i)} E$ is obtained by attaching the root of E to leaf $f_D(i)$ of D , “ e ” denotes the new edge, and

$$f_{D \circ E}(j) = \begin{cases} f_D(j), & 1 \leq j < i, \\ f_E(j - i + 1), & i \leq j < i + l, \\ f_D(j - l + 1), & i + l \leq j \leq k + l - 1. \end{cases}$$

For a justification of the sign $(-1)^\epsilon$, refer to Equations (A.1), (A.2), (A.4), and Definition A.2 in Appendix A.1.

Remark 2.3. We remark, that the S_n action may be used to arrange the coloring $\mathbf{x} \times \mathbf{y}$ in (iii) above in the cyclic order starting with the color 2 at the leftmost leaf. With this, an algebra over $C_* \hat{\mathcal{A}}$ may be represented by inner product diagrams via maps $\rho_{j', j''} : M \otimes A^{\otimes j'} \otimes M \otimes A^{\otimes j''} \rightarrow R$. For more on algebras over $C_* \hat{\mathcal{A}}$, see Appendix A.1.

We need the following “metric refinement” of $C_* \hat{\mathcal{A}}$ generated by diagrams whose edges are labeled either m (metric) or n (non-metric):

Definition 2.4. The **three-colored operad**

$$Q_* \hat{\mathcal{A}} = \bigoplus_{\substack{\mathbf{x} \times \mathbf{y} \in \mathbb{Z}_3^{n+1} \\ n \geq 1}} Q_* \hat{\mathcal{A}}_{\mathbf{y}}^{\mathbf{x}},$$

is the graded R -module generated by tuples (D, f, g, ω) modulo $(D, f, g, -\omega) = -(D, f, g, \omega)$, where D and f are as in Definition 2.2 and $g : \mathcal{E}(D) \rightarrow \{m, n\}$ labels the edges in D (if D is a corolla, g is the empty map). The **metric edges** of D form the set $\mathcal{M}(D) = g^{-1}(m)$; all other edges are **non-metric**. If $\mathcal{M}(D) = \{e_1, \dots, e_l\}$, an **orientation** of D is a formal skew-commutative product $\omega = e_{i_1} \wedge \dots \wedge e_{i_l}$, and the **degree** $|(D, f, g, \omega)| := \#\mathcal{M}(D)$. **Units** are inherited from $C_* \hat{\mathcal{A}}$ and the **boundary** is given by

$$\partial_Q(D, f, g, e_{i_1} \wedge \dots \wedge e_{i_l}) :=$$

$$\sum_{j=1}^l (-1)^j \left[(D/e_{i_j}, f, g/e_{i_j}, e_{i_1} \wedge \cdots \wedge \hat{e}_{i_j} \cdots \wedge e_{i_l}) - (D_{e_{i_j}}, f, g_{e_{i_j}}, e_{i_1} \wedge \cdots \wedge \hat{e}_{i_j} \cdots \wedge e_{i_l}) \right],$$

where $g/e_{i_j}(e) = g(e)$ if $e \neq e_{i_j}$, $D_{e_{i_j}}$ is obtained from D by relabeling e_{i_j} non-metric (n), and $g_{e_{i_j}}$ is the corresponding relabeling. It is straightforward to check that $\partial_Q^2 = 0$. This time the S_k -**action** is given by $\sigma \cdot (D, f, g, \omega) = (D, f \circ \sigma, g, \omega)$, and the **coloring** of $(D, f, g, \omega) \in Q_*\hat{\mathcal{A}}_y^{\mathbf{x}}$ is the pair $\mathbf{x} \times y$. Given generators (D, f_D, g_D, ω_D) and (E, f_E, g_E, ω_E) , define the i^{th} **operadic composition** $(D, f_D, g_D, \omega_D) \circ_i (E, f_E, g_E, \omega_E)$ to be zero unless the root of E and the i^{th} leaf of D have the same color, in which case

$$(D, f_D, g_D, \omega_D) \circ_i (E, f_E, g_E, \omega_E) := (D \circ_{f_D(i)} E, f_{D \circ E}, g_{D \circ E}, \omega_D \wedge \omega_E),$$

where $D \circ_{f_D(i)} E$ is defined as in Definition 2.2 and

$$g_{D \circ E}(e) = \begin{cases} n, & e \text{ is the new edge} \\ g_D(e), & e \in \mathcal{E}(D) \\ g_E(e), & e \in \mathcal{E}(E). \end{cases}$$

For comparison, note that the sign prefixes that appear in the formulas defining the S_k -action and \circ_i -composition in $C_*\hat{\mathcal{A}}$, do not appear correspondingly in $Q_*\hat{\mathcal{A}}$. Figure 4 on page 13 displays a graphical representation of the combinatorial relationships among the generators in $Q_*\hat{\mathcal{A}}_0^{2112}$; this clearly illustrates the boundary ∂_Q . As we shall see in the next section, $C_*\hat{\mathcal{A}}$ and $Q_*\hat{\mathcal{A}}$ are operadically quasi-isomorphic.

3. THE MAP $q : C_*\hat{\mathcal{A}} \rightarrow Q_*\hat{\mathcal{A}}$

In this section, we define an operadic map $q : C_*\hat{\mathcal{A}} \rightarrow Q_*\hat{\mathcal{A}}$ and show that it is a quasi-isomorphism. Our proof depends on the fact that pairahedra are contractible. Let ω_B^{std} denote the standard orientation on a binary diagram $B \in C_0\hat{\mathcal{A}}$ defined in Appendix A.2, and let m denote the constant map $g(e) = m$. We remark that a “binary inner product diagram” is an inner product diagram whose (empty) root has valence 2 and whose other vertices have valence 3.

Definition 3.1. Define $q : C_*\hat{\mathcal{A}} \rightarrow Q_*\hat{\mathcal{A}}$ as follows:

- (i) On units, define q to be the identity.
- (ii) On a corolla $(c, f_{\circlearrowleft}, +1) \in C_*\hat{\mathcal{A}}_y^{\mathbf{x}}$, define

$$q(c, f_{\circlearrowleft}, +1) = \sum_{B \in C_0\hat{\mathcal{A}}_y^{\mathbf{x}}} (B, f_{\circlearrowleft}, m, \omega_B^{\text{std}}).$$

- (iii) Decompose a generator $(D, f, \omega) \in C_*\hat{\mathcal{A}}$ as a \circ_i -composition of corollas, and define $q(D, f, \omega)$ by extending S_k -equivariantly and \circ_i -multiplicatively, *i.e.*,

$$\begin{aligned} q\left(\sigma \cdot (D, f, \omega)\right) &= \sigma \cdot q(D, f, \omega); \\ q\left((E, f, \omega) \circ_i (E', f', \omega')\right) &= q(E, f, \omega) \circ_i q(E', f', \omega'). \end{aligned}$$

This extension is well-defined since $C_*\hat{\mathcal{A}}$ is freely generated by corollas $(c, f_{\circlearrowleft}, +1)$ (modulo the relation $(\cdots, -\omega) = -(\cdots, \omega)$).

By definition, q respects units, the S_k -action, and \circ_i -composition. And furthermore:

Proposition 3.2. *The map $q : C_*\hat{\mathcal{A}} \rightarrow Q_*\hat{\mathcal{A}}$ is a chain map.*

Proof. Since ∂_C and ∂_Q respect S_k -actions and act as derivations of \circ_i , it is sufficient to check the result on a corolla $(c, f_\circ, +1) \in C_*\hat{\mathcal{A}}_y^x$:

$$\begin{aligned}
 q(\partial_C(c, f_\circ, +1)) &= \sum_{D/e=c} q(D, f_\circ, e) \\
 &= \sum_{\substack{D/e=c, \\ (D, f_\circ, e) = (-1)^{\epsilon_1} \sigma \cdot [(c', f'_\circ, 1) \circ_j (c'', f''_\circ, 1)] \\ (c', f'_\circ, 1) \in C_*\hat{\mathcal{A}}_{y'}^x; (c'', f''_\circ, 1) \in C_*\hat{\mathcal{A}}_{y''}^x}} (-1)^{\epsilon_1} \sigma \cdot [q(c', f'_\circ, 1) \circ_j q(c'', f''_\circ, 1)] \\
 &= \sum_{\substack{B' \in C_0\hat{\mathcal{A}}_{y'}^x \\ B'' \in C_0\hat{\mathcal{A}}_{y''}^x}} (-1)^{\epsilon_1} \sigma \cdot [(B', f'_\circ, m, \omega_{B'}^{\text{std}}) \circ_j (B'', f''_\circ, m, \omega_{B''}^{\text{std}})] \\
 &= \sum_{\substack{(B, f_\circ, g, \omega_j) \in Q_*\hat{\mathcal{A}}_y^x \\ \#g^{-1}(n)=1}} (-1)^{\epsilon_2}(B, f_\circ, g, \omega_j),
 \end{aligned}$$

where ϵ_2 is a function of ϵ_1 , and both signs are computed in Appendix A.3. The last expression is summed over all binary diagrams B with exactly one non-metric edge (the one coming from the composition \circ_j) and ω_j is the induced orientation. On the other hand,

$$\begin{aligned}
 (3.1) \quad \partial_Q(q(c, f_\circ, +1)) &= \sum_{B \in C_0\hat{\mathcal{A}}_y^x} \partial_Q(B, f_\circ, m, \omega_B^{\text{std}} = e_1 \wedge \cdots \wedge e_k) \\
 &= \sum_B \sum_{e_i} (-1)^i \left[(B/e_i, f_\circ, m/e_i, \omega_{B/e_i}^{\hat{e}_i}) - (B_{e_i}, f_\circ, g_{e_i}, \omega_{B_{e_i}}^{\hat{e}_i}) \right],
 \end{aligned}$$

where $\omega_B^{\hat{e}_i} = e_1 \wedge \cdots \wedge \hat{e}_i \wedge \cdots \wedge e_k$. First, we claim that the “ B/e_i ” terms cancel. To see this, note that if e_i is an edge of a binary diagram B , there is second binary diagram B' and an edge e' in B' such that $B'/e' = B/e_i$. In fact, B and B' are related by one of the 6 local moves depicted in Definition 4.1 (if $B < B'$, obtain B/e_i by collapsing the edges within the two circles). Thus for purposes of orientation, we may symbolically identify e' with e_i and express their standard orientations as $\omega_{B'}^{\text{std}} = e_1 \wedge \cdots \wedge e_i \wedge \cdots \wedge e_k$ and $\omega_{B'}^{\text{std}} = -e_1 \wedge \cdots \wedge e_i \wedge \cdots \wedge e_k$. Consequently, each “ B/e_i ” term appears twice with opposite signs. Formula (3.1) now simplifies to

$$\partial_Q(q(c, f_\circ, 1)) = \sum_B \sum_{e_i} (-1)^{i+1} (B_{e_i}, f_\circ, g_{e_i}, \omega_{B_{e_i}}^{\hat{e}_i}) = q(\partial_C(c, f_\circ, 1)),$$

summed over all binary diagrams B with exactly one non-metric edge e_i ; the fact that $(-1)^{i+1} \omega_{B_{e_i}}^{\hat{e}_i} = (-1)^{\epsilon_2} \omega_j$ is verified in Appendix A.3. \square

The fact that q is a quasi-isomorphism follows from the next proposition.

Proposition 3.3. *The polytopes associated with T_n , $M_{k,l}$, and $I_{k,l}$ are contractible.*

The proof of Proposition 3.3 is technical and appears in Appendix B.

Corollary 3.4. *The map $q : C_*\hat{\mathcal{A}} \rightarrow Q_*\hat{\mathcal{A}}$ is a quasi-isomorphism of operads.*

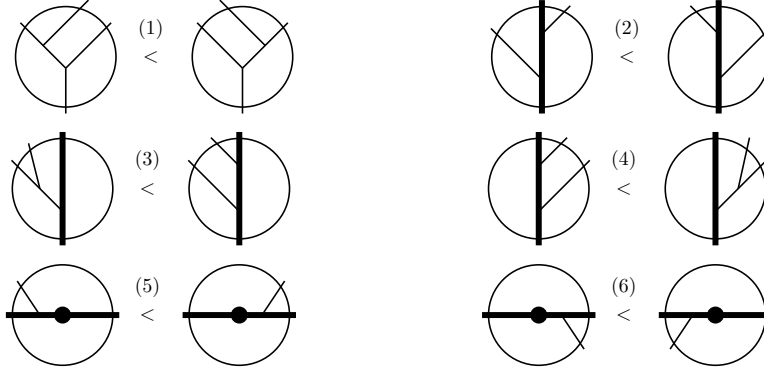
Proof. Since q is a chain map respecting the S_k -action, \circ_i -composition, and units, it is operadic. Furthermore, $q_y^{\mathbf{x}} : C_*\hat{\mathcal{A}}_y^{\mathbf{x}} \rightarrow Q_*\hat{\mathcal{A}}_y^{\mathbf{x}}$ is a quasi-isomorphism for each pair $\mathbf{x} \times y$ by Proposition 3.3 (c.f. [BV]). \square

Geometrically, $C_*\hat{\mathcal{A}}$ is represented by the cellular chains of the various polytopes mentioned above, $Q_*\hat{\mathcal{A}}$ is represented by the cellular chains of an appropriate subdivision, and the morphism q associates each cell of $C_*\hat{\mathcal{A}}$ with the sum of cells in its subdivision (c.f. Figure 4). However, constructing a quasi-inverse of q requires us to make a choice, which we shall do in the next section.

4. THE MAP $p : Q_*\hat{\mathcal{A}} \rightarrow C_*\hat{\mathcal{A}}$

In this section, we define a quasi-inverse p of the morphism q defined in the previous section. Our strategy is to extend the usual Tamari partial ordering on planar binary trees to the set \mathcal{B} of all planar binary diagrams. Given a planar diagram D , let \mathcal{B}_D denote the subposet of \mathcal{B} given by applying all possible sequences of edge insertions to D . Then \mathcal{B}_D has a unique minimal element D_{\min} and maximal element D_{\max} (Lemma 4.2), and p applied to a fully metric diagram D is the sum of all diagrams S such that $S_{\max} \leq D_{\min}$, and extending this in the general case S_k -equivariantly and \circ_i -multiplicatively (see Definition 4.4).

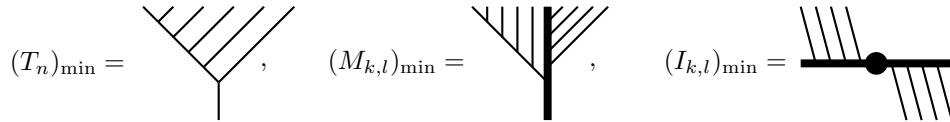
Definition 4.1. A pair of binary diagrams $(B_1, B_2) \in \mathcal{B} \times \mathcal{B}$ is an **edge-pair** if B_1 and B_2 differ only within a single neighborhood in one of the following six possible ways:



The set of all edge-pairs (B_1, B_2) generate a partial order “ \leq ” on \mathcal{B} ; for a proof see Appendix C.

Lemma 4.2. *The subposet \mathcal{B}_D has a unique minimal element D_{\min} and maximal element D_{\max} .*

Proof. Applying all possible sequences of edge insertions to a corolla c generates the subposet \mathcal{B}_c of binary diagrams with unique minimal and maximal elements of the following types:



$$(T_n)_{\max} = \begin{array}{c} \diagup \quad \diagdown \\ \diagup \quad \diagdown \\ \diagup \quad \diagdown \\ \diagup \quad \diagdown \\ | \end{array}, \quad (M_{k,l})_{\max} = \begin{array}{c} \diagup \quad \diagdown \\ \diagup \quad \diagdown \\ \diagup \quad \diagdown \\ \diagup \quad \diagdown \\ | \end{array}, \quad (I_{k,l})_{\max} = \begin{array}{c} \diagup \quad \diagdown \\ \diagup \quad \diagdown \\ \diagup \quad \diagdown \\ \diagup \quad \diagdown \\ \bullet \end{array}$$

Given a diagram $D \in \mathcal{B}$, there is always a sequence of inequalities in \mathcal{B}_D from D_{\min} to D_{\max} . For example,

$$\begin{array}{c} \begin{array}{c} \diagup \quad \diagdown \\ \diagup \quad \diagdown \\ \diagup \quad \diagdown \\ \diagup \quad \diagdown \\ \bullet \end{array} <^{(2)} \begin{array}{c} \diagup \quad \diagdown \\ \diagup \quad \diagdown \\ \diagup \quad \diagdown \\ \diagup \quad \diagdown \\ \bullet \end{array} <^{(5),(2),(6)} \begin{array}{c} \diagup \quad \diagdown \\ \diagup \quad \diagdown \\ \diagup \quad \diagdown \\ \diagup \quad \diagdown \\ \bullet \end{array} \\ <^{(1)} \begin{array}{c} \diagup \quad \diagdown \\ \diagup \quad \diagdown \\ \diagup \quad \diagdown \\ \diagup \quad \diagdown \\ \bullet \end{array} <^{(3)} \begin{array}{c} \diagup \quad \diagdown \\ \diagup \quad \diagdown \\ \diagup \quad \diagdown \\ \diagup \quad \diagdown \\ \bullet \end{array} \end{array}$$

Since every diagram D decomposes as a \circ_i -composition of corollas, the conclusion follows. \square

Remark 4.3. The six local inequalities in Definition 4.1 define one of 2^6 such local systems, some of which fail to generate a partial order on \mathcal{B} . Of those that do, some fail to satisfy the conclusion of Lemma 4.2. However, any partial order generated by one of these local systems satisfying the conclusion of Lemma 4.2 can be used to construct the desired quasi-inverse p .

We are ready to define the operadic quasi-inverse $p : Q_*\hat{\mathcal{A}} \rightarrow C_*\hat{\mathcal{A}}$. We shall refer to a diagram with strictly metric edges as a *fully metric* diagram.

Definition 4.4. Define $p : Q_*\hat{\mathcal{A}} \rightarrow C_*\hat{\mathcal{A}}$ on generators as follows:

- (i) On units, define p to be the identity.
- (ii) On a fully metric diagram $(D, f_\circ, m, \omega_D) \in Q_k\hat{\mathcal{A}}_y^*$, define

$$p(D, f_\circ, m, \omega_D) = \sum_{\substack{(S, f_\circ, \omega(S, D)) \in C_k\hat{\mathcal{A}}_y^* \\ S_{\max} \leq D_{\min}}} (S, f_\circ, \omega(S, D)),$$

where $\omega(S, D)$ is the induced orientation defined in A.2.

- (iii) Decompose a generator $(D, f, g, \omega) \in Q_*\hat{\mathcal{A}}$ with non-metric edges as a \circ_i -composition of fully metric diagrams, and define $p(D, f, g, \omega)$ by extending S_k -equivariantly and \circ_i -multiplicatively, *i.e.*,

$$\begin{aligned} p(\sigma \cdot (D, f, g, \omega)) &= \sigma \cdot (D, f, g, \omega), \\ p((E, f, g, \omega) \circ_i (E', f', g', \omega')) &= p(E, f, g, \omega) \circ_i p(E', f', g', \omega'). \end{aligned}$$

Lemma 4.5. Let $(c, f, g, 1) \in Q_*\hat{\mathcal{A}}$ be a corolla, let $(B, f, m, \omega_B^{std}) \in Q_*\hat{\mathcal{A}}$ be a fully metric binary diagram, and let $\omega(c_{\min}, c)$ be the orientation of c_{\min} given by Equation (A.5) in A.2. Then

- (i) $p(c, f, g, 1) = (c_{\min}, f, \omega(c_{\min}, c))$.
- (ii) $p(B, f, m, \omega_B^{std}) = \begin{cases} (c, f, 1), & \text{if } B = c_{\max} \\ 0, & \text{otherwise.} \end{cases}$

Proof. (i) Let $(S, f, \omega) \in C_*\hat{\mathcal{A}}$ be a summand of $p(c, f, g, 1)$. Then $|(S, f, \omega)| = |(c, f, g, 1)| = 0$, which implies $\#\mathcal{L}(S) = \#\mathcal{E}(S) + 2$. Thus S is a binary diagram and $S = S_{\max}$. Since c is a corolla, $S = S_{\max} \leq c_{\min}$ implies $S = c_{\min}$; hence $p(c, f, g, 1) = (c_{\min}, f, \omega(c_{\min}, c))$.

(ii) Let $(B, f, m, \omega_B^{\text{std}}) \in Q_k\hat{\mathcal{A}}$ be a fully metric binary diagram and let $(S, f, \omega) \in C_k\hat{\mathcal{A}}$ be a summand of $p(B, f, m, \omega_B^{\text{std}})$. Then $B = B_{\min}$ has $k + 2$ leaves and k strictly metric edges so that $k = |(B, f, m, \omega_B^{\text{std}})| = |(S, f, \omega)| = (k + 2) - \#\mathcal{E}(S) - 2$. But $\#\mathcal{E}(S) = 0$ implies $S = c$ is a corolla. The condition $c_{\max} \leq B_{\min} = B$ shows that when B is not a maximum, $p(B, f, m, \omega_B^{\text{std}}) = 0$; otherwise $p(B, f, m, \omega_B^{\text{std}}) = (c, f, +1)$ (the fact that $\omega(c, c_{\max}) = +1$ is verified in Equation (A.6) in A.2. \square)

Proposition 4.6. *The map $p : Q_*\hat{\mathcal{A}} \rightarrow C_*\hat{\mathcal{A}}$ is a chain map.*

A rather lengthy proof of Proposition 4.6 appears in Appendix D.

Proposition 4.7. *The composition $pq = \text{Id}_{C_*\hat{\mathcal{A}}}$, and there is a chain homotopy from the identity $\text{Id}_{Q_*\hat{\mathcal{A}}}$ to the composition qp . Thus, p and q are operadic chain homotopy equivalences.*

Proof. Since p and q respect \circ_i -compositions and $C_*\hat{\mathcal{A}}$ is generated by \circ_i -compositions of corollas, it is sufficient to check pq on a corolla $(c, f, 1) \in C_*\hat{\mathcal{A}}_y^x$. With Lemma 4.5 (ii), we calculate

$$p(q(c, f, 1)) = \sum_{B \in C_0\hat{\mathcal{A}}_y^x} p(B, f, m, \omega_B^{\text{std}}) = p(c_{\max}, f, m, \omega_{c_{\max}}^{\text{std}}) = (c, f, 1).$$

On the other hand, we construct a chain homotopy $S : Q_*\hat{\mathcal{A}} \rightarrow Q_*\hat{\mathcal{A}}$, such that $\partial_Q S + S\partial_Q = qp - \text{Id}_{Q_*\hat{\mathcal{A}}}$. The chain homotopy $S : Q_n\hat{\mathcal{A}} \rightarrow Q_{n+1}\hat{\mathcal{A}}$ is defined by induction on the degree n . For $n = 0$, and the corolla $(c, f, g, 1) \in Q_0\hat{\mathcal{A}}$, Lemma 4.5(i) shows that

$$q(p(c, f, g, 1)) = q(c_{\min}, f, \omega(c_{\min}, c)) = (c_{\min}, f, n, 1),$$

where n is the constant non-metric assignment. The last sign follows from Equation (A.5), $\omega(c_{\min}, c) = \xi_{c_{\min}}$, and the description of $\xi_{c_{\min}}$ given in Remark A.8. Since, by Proposition 3.3, all pairahedra are contractible, we can find a path $S(c, f, g, 1) \in Q_1\hat{\mathcal{A}}$ with boundary endpoints $(qp)(c, f, g, 1) = (c_{\min}, f, n, 1)$ and $(c, f, g, 1)$, so that with $\partial_Q(c, f, g, 1) = 0$, we have:

$$(\partial_Q S + S\partial_Q)(c, f, g, 1) = (qp - \text{Id}_{Q_*\hat{\mathcal{A}}})(c, f, g, 1).$$

Note that qp is \circ_i -multiplicative and we extend S to all of $Q_0\hat{\mathcal{A}}$ as an (Id, qp) -derivation. With this, $\partial_Q S + S\partial_Q = qp - \text{Id}_{Q_*\hat{\mathcal{A}}}$ holds on all of $Q_0\hat{\mathcal{A}}$.

Inductively, assume that for all $k < n$, the map S has been extended as a chain homotopy from $\text{Id}_{Q_*\hat{\mathcal{A}}}$ to qp on $Q_k\hat{\mathcal{A}}$. Then, on $Q_n\hat{\mathcal{A}}$,

$$\begin{aligned} \partial_Q (qp - \text{Id}_{Q_*\hat{\mathcal{A}}} - S\partial_Q) &= (qp - \text{Id}_{Q_*\hat{\mathcal{A}}}) \partial_Q - \partial_Q S \partial_Q \\ &= (qp - \text{Id}_{Q_*\hat{\mathcal{A}}} - \partial_Q S) \partial_Q = S \partial_Q^2 = 0. \end{aligned}$$

Thus, since the pairahedra are contractible, $(qp - \text{Id}_{Q_*\hat{\mathcal{A}}} - S\partial_Q)(D, f, m, \omega) \in Q_n\hat{\mathcal{A}}$ is a boundary for every $(D, f, m, \omega) \in Q_n\hat{\mathcal{A}}$. Choose $(D', f', g', \omega') \in Q_{n+1}\hat{\mathcal{A}}$ such

that $\partial_Q(D', f', g', \omega') = (qp - \text{Id}_{Q_*\hat{A}} - S\partial_Q)(D, f, m, \omega)$ and define $S(D, f, m, \omega) = (D', f', g', \omega')$. Then $(qp - \text{Id}_{Q_*\hat{A}} - S\partial_Q - \partial_Q S)(D, f, m, \omega) = 0$, so that $S\partial_Q + \partial_Q S = qp - \text{Id}_{Q_*\hat{A}}$ holds on $Q_n\hat{A}$. Hence $S : qp \simeq \text{Id}_{Q_*\hat{A}}$. \square

5. THE DIAGONAL $\Delta_C : C_*\hat{A} \rightarrow C_*\hat{A} \otimes C_*\hat{A}$

Let I^n denote the standard n -cube, let $I = \sqcup_n I^n$ and let $C_*(I)$ denote cellular chains. The Serre diagonal $\Delta_I : C_*(I) \rightarrow C_*(I) \otimes C_*(I)$ acts on each cube I^n of the cubical complex $Q_*\hat{A}$ and induces a coassociative diagonal Δ_Q on $Q_*\hat{A}$. In turn, Δ_Q induces a non-coassociative diagonal Δ_C on $C_*\hat{A}$ via p and q .

Given a generator $(D, f, g, \omega) \in Q_*\hat{A}$ and a subset $X \subseteq \{e_1, \dots, e_k\} = g^{-1}(m)$, let $\bar{X} = g^{-1}(m) \setminus X$ and $\rho(X) = \#\{(e_i, e_j) \in X \times \bar{X} \mid i < j\}$. Consider the following related generators:

- $(D/X, f, g_{D/X}, \omega_{D/X})$, where D/X is obtained from D by contracting the edges of X , $g_{D/X}$ is the labeling induced by g , and $\omega_{D/X}$ is the orientation obtained from ω by deleting all factors in X ;
- $(D_{\bar{X}}, f, g_{D_{\bar{X}}}, \omega_{D_{\bar{X}}})$, where $D_{\bar{X}}$ is obtained from D by reversing labels on the edges in \bar{X} , $g_{D_{\bar{X}}}$ agrees with g except on \bar{X} , and $\omega_{D_{\bar{X}}}$ is the orientation obtained from ω by deleting all factors in \bar{X} .

Definition 5.1. Define $\Delta_Q : Q_*\hat{A} \rightarrow Q_*\hat{A} \otimes Q_*\hat{A}$ on generators by

$$\Delta_Q(D, f, g, \omega) = \sum_{X \subseteq g^{-1}(m)} (-1)^{\rho(X)} (D/X, f, g_{D/X}, \omega_{D/X}) \otimes (D_{\bar{X}}, f, g_{D_{\bar{X}}}, \omega_{D_{\bar{X}}}).$$

In particular, if c is a corolla, then $\Delta_Q(c, f, g, 1) = (c, f, g, 1) \otimes (c, f, g, 1)$, where g is the empty map.

The restriction of Δ_Q to the submodule \mathcal{A}_∞ generated by metric planar rooted trees defines a (strictly coassociative) DG coalgebra structure on \mathcal{A}_∞ that commutes with the operadic structure, see [MS, Proposition 5.1].

Definition 5.2. Define $\Delta_C : C_*\hat{A} \rightarrow C_*\hat{A} \otimes C_*\hat{A}$ to be the composition

$$C_*\hat{A} \xrightarrow{q} Q_*\hat{A} \xrightarrow{\Delta_Q} Q_*\hat{A} \otimes Q_*\hat{A} \xrightarrow{p \otimes p} C_*\hat{A} \otimes C_*\hat{A}.$$

To simplify notation, we sometimes abuse notation and write $D \in C_*\hat{\mathcal{A}}_y^x$ when we mean (D, f, ω_D) .

Proposition 5.3. *On a corolla $(c, f, +1) \in C_k\hat{\mathcal{A}}_y^x$ we have*

$$\Delta_C(c, f, +1) = \sum_{\substack{S \otimes T \in C_i\hat{\mathcal{A}}_y^x \otimes C_j\hat{\mathcal{A}}_y^x \\ S_{\max} \leq T_{\min} \\ i+j=k}} \pm (S, f, \omega_S) \otimes (T, f, \omega_T).$$

Proof. We evaluate the composition $(p \otimes p) \circ \Delta_Q \circ q$:

$$\begin{aligned} \Delta_C(c, f, +1) &= (p \otimes p)\Delta_Q(q(c, f, +1)) \\ &= \sum_{B \in C_0\hat{\mathcal{A}}_y^x} (p \otimes p)\Delta_Q(B, f, m, \omega_B^{\text{std}}) \end{aligned}$$

$$= \sum_{\substack{B \in C_0 \hat{\mathcal{A}}_y^{\times} \\ X \subseteq \mathcal{E}(B)}} \pm p(B/X, f, g_{B/X}, \omega_{B/X}) \otimes p(B_{\bar{X}}, f, g_{B_{\bar{X}}}, \omega_{B_{\bar{X}}}).$$

To evaluate $p(B_{\bar{X}}, f, g_{B_{\bar{X}}}, \omega_{B_{\bar{X}}})$, note that the non-metric edges of the binary diagram B are exactly the edges in $\bar{X} = \{e_1, \dots, e_{k-1}\}$, and B decomposes as a \circ_i -composition of fully metric binary diagrams B_1, \dots, B_k along the edges of \bar{X} :

$$(B_{\bar{X}}, f, g_{B_{\bar{X}}}, \omega_{B_{\bar{X}}}) = \pm \sigma \cdot [(B_1, f_1, m, \omega_1) \circ_{e_1} \cdots \circ_{e_{k-1}} (B_k, f_k, m, \omega_k)]$$

(such decompositions are unique up to operadic associativity). Since B_i is fully metric, Lemma 4.5 implies that $p(B_i, f_i, m, \omega_i)$ is a corolla if B_i is maximal and vanishes otherwise. Hence if $p(B_{\bar{X}}, f, g_{B_{\bar{X}}}, \omega_{B_{\bar{X}}}) \neq 0$, each B_i is maximal and $p(B_{\bar{X}}, f, g_{B_{\bar{X}}}, \omega_{B_{\bar{X}}}) = \pm (B/X, f, \omega_{B/X})$. Furthermore, if $(T, f, \omega_T) \in C_* \hat{\mathcal{A}}_y^{\times}$, there is a unique B with maximal B_i 's such that $T = B/X$. Consequently,

$$\begin{aligned} \Delta_C(c, f, 1) &= \sum_{\substack{B \in C_0 \hat{\mathcal{A}}_y^{\times} \\ X \subseteq \mathcal{E}(B) \\ \text{all } B_i \text{ maximal}}} \pm p(B/X, f, g_{B/X}, \omega_{B/X}) \otimes (B/X, f, \omega_{B/X}) \\ &= \sum_{\substack{S \otimes T \in C_i \hat{\mathcal{A}}_y^{\times} \otimes C_j \hat{\mathcal{A}}_y^{\times} \\ S_{\max} \leq T_{\min} \\ i+j=k}} \pm (S, f, \omega_S) \otimes (T, f, \omega_T). \end{aligned}$$

□

Remark 5.4. In [MS, Proposition 5.1], Markl and Shnider proved the special case of Proposition 5.3 with Δ_C restricted to the submodule \mathcal{A}_∞ generated by planar rooted trees. Since Δ_Q is induced by the Serre diagonal on I^n , it is strictly coassociative on $Q_* \hat{\mathcal{A}}$. However, Δ_C is not coassociative. In fact, Markl and Shnider also remarked that Δ_C cannot be chosen to be coassociative on \mathcal{A}_∞ . Nevertheless, this structure is homotopy coassociative, and the formula for Δ_C in Proposition 5.3 extends to a \mathcal{A}_∞ -coalgebra structure on $C_* \hat{\mathcal{A}}$ in a natural way (for the special \mathcal{A}_∞ case see [L]).

6. COMPUTATIONS

In this section, we make explicit computations and remarks about the diagonal $\Delta_C : C_* \hat{\mathcal{A}} \rightarrow C_* \hat{\mathcal{A}} \otimes C_* \hat{\mathcal{A}}$ in various situations. In Example 6.1 we calculate the diagonal of $I_{2,0}$, and in Example 6.2 we make some general remarks about the diagonal as it would appear for a cyclic \mathcal{A}_∞ -algebra. Both of these examples are given on the level of operads, and may be transferred to the corresponding statements for homotopy inner products. In Remark 6.3 we comment on the diagonal for strong homotopy inner products in the sense of [C]. In all of these considerations, we ignore signs and always write “+” regardless of orientation.

Example 6.1. To evaluate $\Delta_C = (p \otimes p) \circ \Delta_Q \circ q$ on the corolla $I_{2,0}$, note that

$$q(I_{2,0}) = \begin{array}{c} \diagdown \quad \diagup \\ \bullet \\ \hline \bullet \end{array} + \begin{array}{c} \diagup \quad \diagdown \\ \bullet \\ \hline \bullet \end{array} + \begin{array}{c} \diagdown \quad \diagup \\ \bullet \\ \hline \bullet \end{array} + \begin{array}{c} \diagup \quad \diagdown \\ \bullet \\ \hline \bullet \end{array} + \begin{array}{c} \diagdown \quad \diagup \\ \bullet \\ \hline \bullet \end{array}$$

is the sum of the five squares in the metric pairahedron pictured in Figure 4. Evaluating the Serre diagonal on each of these squares gives

Applying $p \otimes p$ we obtain

$$\begin{aligned} \Delta_C\left(\begin{array}{c} \diagdown \\ \bullet \\ \diagup \end{array}\right) &= \begin{array}{c} \diagdown \\ \bullet \\ \diagup \end{array} \otimes \begin{array}{c} \diagup \\ \bullet \\ \diagdown \end{array} + \begin{array}{c} \diagdown \diagdown \\ \bullet \\ \diagup \end{array} \otimes \begin{array}{c} \diagdown \\ \bullet \\ \diagup \end{array} + \begin{array}{c} \diagdown \\ \bullet \\ \diagup \end{array} \otimes \begin{array}{c} \diagdown \diagdown \\ \bullet \\ \diagup \end{array} \\ &+ \begin{array}{c} \diagdown \diagdown \\ \bullet \\ \diagup \end{array} \otimes \begin{array}{c} \diagdown \diagdown \\ \bullet \\ \diagup \end{array} + \left(\begin{array}{c} \diagdown \\ \bullet \\ \diagup \end{array} + \begin{array}{c} \diagup \\ \bullet \\ \diagdown \end{array} \right) \otimes \begin{array}{c} \diagdown \diagdown \\ \bullet \\ \diagup \end{array}. \end{aligned}$$

Note that if D is a right-factor in a non-primitive term of $\Delta_C(I_{2,0})$, the set of all left-hand factors that pair off with D in $\Delta_C(I_{2,0})$ form a path from the minimal vertex of $I_{2,0}$ to the maximal vertex of $I_{2,0}$ (see Figure 5).

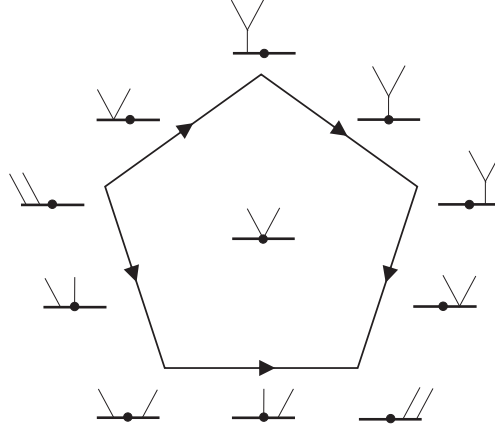


FIGURE 5. The vertex poset of $I_{2,0}$.

Example 6.2. Let us calculate Δ_C in low dimensions as it would appear in the setting of a *cyclic* A_∞ -algebra. In this case, the corolla $I_{k,l}$ corresponds to a zero map whenever $k+l > 0$, and the non-trivial inner product diagram $I_{0,0}$ consists of two thick horizontal edges joined at a common vertex. Thus we compute $\Delta_C(c) = \sum \pm S \otimes T$ by summing over all diagrams for inner products S and T such that $S_{\max} \leq T_{\min}$ (see Proposition 5.3), and we will only keep track of terms involving $I_{0,0}$, that is we mod out by terms involving higher inner products $I_{k,l}$ with $k+l > 0$. The results below can be obtained as in Example 6.1, and subsequently removing all solutions involving higher inner products $I_{k,l}$ with $k+l > 0$. However, these calculations are much more involved than those in Example 6.1, and we leave them as an exercise to the reader. We obtain the following:

$$\begin{aligned} \Delta_C(I_{0,0}) &= I_{0,0} \otimes I_{0,0}, \\ \Delta_C(I_{1,0}) &= \Delta_C(I_{0,1}) = \Delta_C(I_{1,1}) = 0, \\ \Delta_C(I_{2,0}) &\equiv \begin{array}{c} \diagdown \\ \bullet \\ \diagup \end{array} \otimes \begin{array}{c} \diagdown \\ \bullet \\ \diagup \end{array} \pmod{\{I_{k,l} : k+l > 0\}}. \end{aligned}$$

Note that $\Delta_C(I_{2,0})$ corresponds to the chain homotopy $\varrho_{2,0}$ mentioned in the introduction. More precisely, in the introduction, we considered the canonical example of the ∞ -bimodule A over the A_∞ -algebra A as defined in the appendix, cf. Equation (A.3), whose ∞ -bimodule structure $\lambda_{j',j''}$ is given by the A_∞ -algebra structure $\mu_{j'+j''+1}$, and similarly for the ∞ -bimodule structure for B .

The above expression is a special case of the following more general formula:

$$\Delta_C(I_{k,l}) = \sum_{r=0}^{k+l} \sum_{i=1}^{p_r} S_i^{(r)} \otimes T_i^{(k+l-r)},$$

where $S_i^{(q)}, T_i^{(q)} \in C_q \hat{\mathcal{A}}$ are of degree q . In the special case of concern in this example, that is for cyclic A_∞ -algebras, the $r = 0$ and $r = k + l$ terms vanish, and the $r = 1$ and $r = k + l - 1$ terms are given by the formula:

$$\begin{aligned} \Delta_C(I_{k,l}) \equiv & \left(\text{diagram with } k \text{ slashes on left} \right) \otimes \left(\text{diagram with } l \text{ slashes on right} + \dots + \text{diagram with } k+l \text{ slashes} \right) \\ & + \left(\text{diagram with } k+l \text{ slashes on left} \right) \otimes \left(\text{diagram with } l \text{ slashes on right} + \dots + \text{diagram with } k+l \text{ slashes} \right) \\ & + \sum_{r=2}^{k+l-2} \sum_i S_i^{(r)} \otimes T_i^{(k+l-r)} \\ & + \left(\text{diagram with } l \text{ slashes on left} + \dots + \text{diagram with } k+l \text{ slashes} \right) \otimes \left(\text{diagram with } k \text{ slashes on right} \right) \\ & + \left(\text{diagram with } l \text{ slashes on left} + \dots + \text{diagram with } k+l \text{ slashes} \right) \otimes \left(\text{diagram with } k \text{ slashes on right} \right) \\ & \pmod{\{I_{k,l} : k+l > 0\}}. \end{aligned}$$

Computing Δ_C in general requires more work, as the formula for $\Delta_C(I_{4,0})$ shows:

$$\begin{aligned} \Delta_C(I_{2,1}) & \equiv \left(\text{diagram with } 1 \text{ slash on left} \right) \otimes \left(\text{diagram with } 1 \text{ slash on right} \right) + \left(\text{diagram with } 1 \text{ slash on left} \right) \otimes \left(\text{diagram with } 1 \text{ slash on right} \right) \pmod{\{I_{k,l} : k+l > 0\}}, \\ \Delta_C(I_{3,0}) & \equiv \left(\text{diagram with } 3 \text{ slashes on left} \right) \otimes \left(\text{diagram with } 0 \text{ slashes on right} \right) \\ & + \left(\text{diagram with } 2 \text{ slashes on left} + \text{diagram with } 1 \text{ slash on left} \right) \otimes \left(\text{diagram with } 0 \text{ slashes on right} \right) \pmod{\{I_{k,l} : k+l > 0\}}, \\ \Delta_C(I_{4,0}) & \equiv \left(\text{diagram with } 4 \text{ slashes on left} \right) \otimes \left(\text{diagram with } 0 \text{ slashes on right} \right) \\ & + \left(\text{diagram with } 3 \text{ slashes on left} \right) \otimes \left(\text{diagram with } 0 \text{ slashes on right} \right) + \left(\text{diagram with } 2 \text{ slashes on left} \right) \otimes \left(\text{diagram with } 0 \text{ slashes on right} \right) \\ & + \left(\text{diagram with } 2 \text{ slashes on left} \right) \otimes \left(\text{diagram with } 0 \text{ slashes on right} \right) + \left(\text{diagram with } 1 \text{ slash on left} \right) \otimes \left(\text{diagram with } 0 \text{ slashes on right} \right) \\ & + \left(\text{diagram with } 1 \text{ slash on left} \right) \otimes \left(\text{diagram with } 0 \text{ slashes on right} \right) + \left(\text{diagram with } 0 \text{ slashes on left} \right) \otimes \left(\text{diagram with } 0 \text{ slashes on right} \right) \\ & + \left(\text{diagram with } 3 \text{ slashes on left} + \text{diagram with } 2 \text{ slashes on left} + \text{diagram with } 1 \text{ slash on left} \right) \otimes \left(\text{diagram with } 0 \text{ slashes on right} \right) \\ & \pmod{\{I_{k,l} : k+l > 0\}} \end{aligned}$$

Remark 6.3. In Example 6.2 we observed that the tensor product of cyclic A_∞ -algebras is, in general, not cyclic. One could also consider strong homotopy inner products considered by Cho [C], which are cyclic A_∞ -algebras up to homotopy, and ask whether or not the tensor product preserves such structures. In [C, Theorem

5.1], Cho showed that a homotopy inner product transforms into a strong homotopy inner product if and only if it satisfies the following three conditions:

- (1) Skew Symmetry: $\rho_{k,l}(a, \underline{b}, c, \underline{d}) = \pm \rho_{l,k}(c, \underline{d}, a, \underline{b})$,
- (2) Closedness:

$$\rho_{k+l+1,m}(\dots, a, \dots, \underline{b}, \dots, \underline{c}) \pm \rho_{k,l+m+1}(\dots, \underline{a}, \dots, b, \dots, \underline{c}) \\ \pm \rho_{l+m+1,k}(\dots, c, \dots, \underline{a}, \dots, \underline{b}) = 0,$$

- (3) Homological non-degeneracy: $(\rho_{0,0})_*$ is non-degenerate.

For more details on the notation and signs, we refer the reader to [C] or [T2]. Now the symmetrical nature of the definition of Δ_C implies that the tensor product of two skew-symmetric homotopy inner products (satisfying condition (1)) is also skew-symmetric: If S^* denotes the diagram obtained from S by rotating 180° , then $(S^*)_{\max} = (S_{\max})^*$, $(D^*)_{\min} = (D_{\min})^*$, and $S_{\max} \leq D_{\min} \Leftrightarrow (S_{\max})^* \leq (D_{\min})^*$. Furthermore, under reasonable conditions, it is clear that the tensor product of two homologically non-degenerate homotopy inner products (satisfying property (3)) is also homologically non-degenerate. Thus we conjecture that tensor products also preserve property (2), and that the tensor product is closed in the strong homotopy inner product category.

Acknowledgments. We wish to thank Jean-Louis Loday and Jim Stasheff for sharing their thoughts and insights with us during discussions related to this topic.

APPENDIX A. SIGNS

In this appendix we discuss various issues related to the definition and calculation of signs in this paper. To begin, we review the signs in an A_∞ -algebra with homotopy inner products, define the canonical orientation of a binary diagram, and check the signs in Proposition 3.2.

A.1. Signs in an A_∞ -algebra with homotopy inner product. Let $A = \bigoplus_{i \in \mathbb{Z}} A_i$ be a differential graded R -module (DGM) with differential $d : A \rightarrow A$ of degree $+1$. The tensor product of DGM maps f and g satisfies $(f \otimes g)(a \otimes b) = (-1)^{|g| \cdot |a|} f(a) \otimes g(b)$. If $(A^1, d^1), \dots, (A^{k+1}, d^{k+1})$ are DGMs, the induced differential d on $A^1 \otimes \dots \otimes A^k$ is given by

$$d = \sum_{i=1}^k \mathbf{1}^{\otimes(i-1)} \otimes d^i \otimes \mathbf{1}^{\otimes(k-i)},$$

and the induced differential D on $\text{Hom}(A^1 \otimes \dots \otimes A^k, A^{k+1})$ is given by the commutator

$$[D, f] = d^{k+1} f - (-1)^{|f|} f d.$$

An A_∞ -algebra structure on A consists of a family of maps $\{\mu_k : A^{\otimes k} \rightarrow A\}_{k \geq 2}$ such that $|\mu_k| = 2 - k$ and

$$(A.1) \quad [D, \mu_k] = \sum_{j+\ell=k+1} \sum_{i=1}^{k-j+1} (-1)^{i(j+1)+j\ell} \mu_\ell \circ \left(\mathbf{1}^{\otimes(i-1)} \otimes \mu_j \otimes \mathbf{1}^{\otimes(k-j-i+1)} \right).$$

Remark A.1. There are various choices of signs in the A_∞ -algebra structure relations. For example, one could define an A_∞ -algebras in terms of maps $\mu'_k : A^{\otimes k} \rightarrow A$ such that

$$[d, \mu'_k] = \sum_{j+\ell-1=k} \sum_{i=1}^{k-j+1} (-1)^{(i-1)\cdot(j+1)+\ell} \cdot \mu'_\ell \circ \left(\mathbf{1}^{\otimes(i-1)} \otimes \mu'_j \otimes \mathbf{1}^{\otimes(k-j-i+1)} \right).$$

The two definitions are related via the relation $\mu'_k = (-1)^{\frac{k(k+1)}{2}+1} \cdot \mu_k$. Note that the simplest signs arise by shifting dimension in A up by 1 and removing all signs. We refer the reader *e.g.* to [T1] and [SU] for details.

An ∞ -bimodule over A consists of a DGM M together with a family of module maps $\{\lambda_{j',j''} : A^{\otimes j'} \otimes M \otimes A^{\otimes j''} \rightarrow M\}$ such that

$$(A.2) \quad [D, \lambda_{k',k''}] = \sum_{j+\ell=k+1} \sum_{i=1}^{k-j+1} (-1)^{i(j+1)+j\ell} \lambda_{\ell',\ell''} \left(\mathbf{1}^{\otimes(i-1)} \otimes q_J \otimes \mathbf{1}^{\otimes(k-j-i+1)} \right),$$

where $k = k' + k'' + 1$, $\ell = \ell' + \ell'' + 1$, and q_J is either $\lambda_{j',j''}$ or μ_j , which is determined by the i^{th} to the $(k-j+i)^{\text{th}}$ input in $A^{\otimes k'} \otimes M \otimes A^{\otimes k''}$. An important example of an ∞ -bimodule is given by setting $M = A$ and

$$(A.3) \quad \lambda_{j',j''} = \mu_{j'+j''+1}.$$

This example also helps to clarify the signs in the formula above.

Finally, given ∞ -bimodule over A , a *homotopy inner product* consists of a family of maps $\{\varrho_{j',j''} : M \otimes A^{\otimes j'} \otimes M \otimes A^{\otimes j''} \rightarrow R\}$, such that

$$(A.4) \quad [D, \varrho_{k',k''}] = \sum_{j'+j''+\ell=k} (-1)^{(j+1)+j\ell+j'(j''+\ell)} \varrho_{\ell',\ell''} \left(\lambda_{j',j''} \otimes \mathbf{1}^{\otimes(k-j'-j''-1)} \right) \underbrace{(\tau_{\#} \circ \dots \circ \tau_{\#})}_{j' \text{ cyclic permut.}} \\ + \sum_{j+\ell-1=k} \sum_{i=2}^{k-j+1} (-1)^{i(j+1)+j\ell} \varrho_{\ell',\ell''} \left(\mathbf{1}^{\otimes(i-1)} \otimes q_J \otimes \mathbf{1}^{\otimes(k-j-i+1)} \right),$$

where $k = k' + k'' + 2$, $\ell = \ell' + \ell'' + 2$, and q_J is either $\lambda_{j',j''}$ or μ_j depending on the inputs. The first line of the formula involves composition in the first position ($i = 1$) after cyclically permuting j' elements from back-to-front, i.e.,

$$\tau_{\#} : A^{\otimes i'} \otimes M \otimes A^{\otimes i''} \otimes M \otimes A^{\otimes i'''+1} \rightarrow A^{\otimes i'+1} \otimes M \otimes A^{\otimes i''} \otimes M \otimes A^{\otimes i'''},$$

then applying $\lambda_{j',j''}$. This cyclical rotation of j' elements gives rise to the additional sign coefficient here.

The signs (A.1), (A.2), and (A.4), which appear in the definitions of an A_∞ -algebra and a homotopy inner product, also appear in the definition of $C_*\hat{\mathcal{A}}$. Let $\mathcal{E}nd_{(A,M,R)}$ denote the endomorphism operad of the triple (A, M, R) . Then under the conventions above, a morphism of operads $C_*\hat{\mathcal{A}} \rightarrow \mathcal{E}nd_{(A,M,R)}$ defines an A_∞ -algebra A with homotopy inner product structure on M , as is evident in the next definition.

Definition A.2. Given an A_∞ -algebra with ∞ -bimodule and homotopy inner product structures $(A, M, R, \{\mu_i\}_i, \{\lambda_{i,j}\}_{i,j}, \{\varrho_{i,j}\}_{i,j})$, define the operad map $F : C_*\hat{\mathcal{A}} \rightarrow \mathcal{E}nd_{(A,M,R)}$ as follows: For a corolla $c = T_i, M_{i,j}$ or $I_{i,j}$ (see Figure 1), the

canonical clockwise assignment f_\circ of inputs (see Figure 3), and the canonical orientation $\omega = +1$ of the empty set of edges, define $F(c, f_\circ, +1)$ to be the structure associated with this corolla, i.e.,

$$F(T_i, f_\circ, +1) = \mu_i, \quad F(M_{i,j}, f_\circ, +1) = \lambda_{i,j}, \quad F(I_{i,j}, f_\circ, +1) = \varrho_{i,j}.$$

For a diagram D with exactly one edge e and the canonical labeling f_\circ , the signs in F are determined by (A.1), (A.2), and (A.4). For example, if $D \in C_* \hat{\mathcal{A}}_1^{11 \cdots 1}$ is a tree and the edge $e = e(i, j)$ determines the subtree T_j attached to T_ℓ at position i , then, from (A.1),

$$F(D, f_\circ, e(i, j)) = d_{e(i,j)}(\mu_k) := (-1)^{i(j+1)+j\ell} \mu_\ell (1^{\otimes i-1} \otimes \mu_j \otimes 1^{\otimes \ell-i}).$$

Similarly, for a general diagram D and any edge $e \in \mathcal{E}(D)$, we have an operation d_e of degree $+1$, and set

$$F(D, f_\circ, e_1 \wedge \cdots \wedge e_r) = d_{e_1} \circ \cdots \circ d_{e_r}(q_J),$$

where q_J is one of the maps $\mu_i, \lambda_{i,j}$, or $\varrho_{i,j}$. When d_e passes a structure map $q'_{J'}$, the usual Koszul sign commutation rule applies: $d_e \circ q'_{J'} = (-1)^{|q'_{J'}|} q'_{J'} \circ d_e$.

Finally, for a non-trivial labeling $f : \{1, \dots, k\} \rightarrow \mathcal{L}(D)$, we uniquely write f as a composition of a permutation $\sigma \in S_k$ and the clockwise labeling, $f = f_\circ \circ \sigma$, and denoting by $\sigma_\#(x_1 \otimes \cdots \otimes x_k) = x_{\sigma^{-1}(1)} \otimes \cdots \otimes x_{\sigma^{-1}(k)}$ a permutation of tensor factors, we set

$$F(D, f_\circ \circ \sigma, \omega) = \text{sgn}(\sigma) \cdot F(D, f_\circ, \omega) \circ \sigma_\#.$$

With this, one can check that the signs appearing in Equation (2.1) make F into an operad map. For example, for $(D, f_\circ, \omega_D) \in C_n \hat{\mathcal{A}}_1^{11 \cdots 1}$, $k = \#\mathcal{L}(D)$, and $(E, id, \omega_E) \in C_m \hat{\mathcal{A}}_1^{11 \cdots 1}$, $l = \#\mathcal{L}(E)$, we have

$$\begin{aligned} & F((D, f_\circ, e_1^D \wedge \cdots \wedge e_{k-n-2}^D) \circ_i (E, f_\circ, e_1^E \wedge \cdots \wedge e_{l-m-2}^E)) \\ &= (-1)^{km+i(l+1)} F(D \circ_i E, f_\circ, e_1^D \wedge \cdots \wedge e_{k-n-2}^D \wedge e_1^E \wedge \cdots \wedge e_{l-m-2}^E \wedge e) \\ &= (-1)^{km+i(l+1)} d_{e_1^D} \circ \cdots \circ d_{e_{k-n-2}^D} \circ d_{e_1^E} \circ \cdots \circ d_{e_{l-m-2}^E} \circ d_e(\mu_{k+l-1}) \\ &= (-1)^{k(m+l)} d_{e_1^D} \circ \cdots \circ d_{e_{k-n-2}^D} \circ d_{e_1^E} \circ \cdots \circ d_{e_{l-m-2}^E} (\mu_k \circ (1^{\otimes i-1} \otimes \mu_l \otimes 1^{\otimes l-j})) \\ &= d_{e_1^D} \circ \cdots \circ d_{e_{k-n-2}^D} (\mu_k \circ (1^{\otimes i-1} \otimes d_{e_1^E} \circ \cdots \circ d_{e_{l-m-2}^E} (\mu_l) \otimes 1^{\otimes l-j})) \\ &= F(D, f_\circ, e_1^D \wedge \cdots \wedge e_{k-n-2}^D) \circ_i F(E, f_\circ, e_1^E \wedge \cdots \wedge e_{l-m-2}^E). \end{aligned}$$

A similar calculation applies in the other cases.

A.2. Orientation on binary trees. In this appendix, we describe the canonical orientation of a binary diagram, either as element of $C_* \hat{\mathcal{A}}$ or as a non-metric element of $Q_* \hat{\mathcal{A}}$. The main ingredient is an extension of Mac Lane's Coherence Theorem [MacL] to homotopy inner products, by which any two paths of binary diagrams are connected via sequences of pentagons, hexagons, and squares.

Definition A.3. A **path of binary diagrams** is a sequence of binary diagrams $\beta = (B_1, \dots, B_n)$ such that (B_i, B_{i+1}) is an edge-pair for all i (see Definition 4.1).

We consider paths up to equivalence, where the equivalence relation is generated by,

$$(\dots, B_{i-1}, B_i, B_{i+1}, \dots) \sim (\dots, B_{i-1}, B_i, \tilde{B}_i, B_i, B_{i+1}, \dots),$$

where \tilde{B}_i is related to B_i by a local move.

For example, the boundaries of the pentagons $T_4, M_{0,3}, M_{1,2}, M_{2,1}, M_{3,0}, I_{2,0}, I_{0,2}$ and the hexagon $I_{1,1}$ are paths for any choice of starting/ending point. Furthermore, two disjoint local moves define a square path (called a *naturality square*) by applying move 1, then move 2, then undoing move 1, and undoing move 2. A *fundamental path* is a naturality square or the boundary paths of one of the aforementioned corollas.

Definition A.4. Two (equivalence classes of) paths are **one-step-connected** if they differ (locally) by a fundamental path. Two paths β_1 and β_m are **connected** if there is a sequence of paths β_1, \dots, β_m such that β_i and β_{i+1} are one-step-connected for all i .

For example, consider a diagram P_1 and a sequence of diagrams $(P_1, P_2, P_3, P_4, P_5, P_1)$ that differ locally from P_1 by a fundamental path, which is the boundary of the Stasheff pentagon. Then the following paths β_1 and β_2 are one-step-connected: $\beta_1 = (B_1, \dots, B_{k-1}, P_1, B_{k+1}, \dots, B_n)$ and $\beta_2 = (B_1, \dots, B_{k-1}, P_1, P_2, P_3, P_4, P_5, P_1, B_{k+1}, \dots, B_n)$.

Lemma A.5 (Coherence Lemma). *Any two paths $\beta = (B_1, \dots, B_n)$ and $\beta' = (B'_1, \dots, B'_{n'})$ such that $B_1 = B'_1$ and $B_n = B'_{n'}$ are connected.*

The lemma can be proved in the same manner as the “associative Coherence Lemma” in [MacL, Section VII.2.]. Thus to define a concept on binary diagrams via paths, it is sufficient to check that the definition is independent of path with respect to fundamental paths. Let us do this for the notion of the standard orientation. First note that each local move from $B \rightsquigarrow B'$ (as given by (1)-(6) in Definition 4.1 with its induced identification of edges) transfers an orientation ω from B to B' by setting $\omega = e_1 \wedge \dots \wedge e_k = -\omega'$. One can check that traversing any of the fundamental paths preserves orientation (see Figure 6 for example).

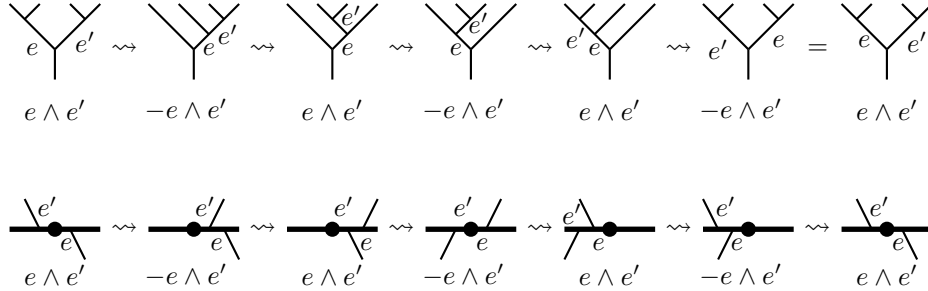


FIGURE 6. Orientation is preserved along boundaries of corollas T_4 (top line) and $I_{1,1}$ (bottom line).

Thus if $\beta = (B, \dots, B')$ is a path from diagram B to diagram B' , an orientation ω on B transfers to an orientation ω_β on B' . And furthermore, Lemma A.5 assures us that ω_β is independent of path since it is preserved along paths coming from fundamental paths. Let us use this idea to define the standard orientation ω_B^{std} on a binary diagram B .

Definition A.6. Let B be a binary diagram of the three types pictured in Figure 7. Define the **standard orientation** ω_B^{std} on B by

$$\omega_B^{\text{std}} := e_1 \wedge \cdots \wedge e_k \in \bigwedge^k \mathcal{E}(B)$$

The standard orientation on a general binary diagram B is induced by any path from one of the diagrams in Figure 7 to B .

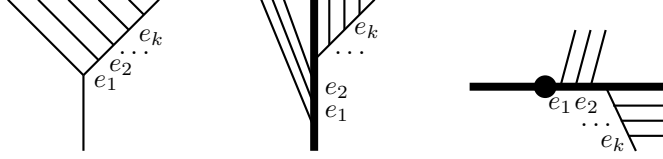


FIGURE 7. Diagrams with standard orientation $e_1 \wedge \cdots \wedge e_k$

Example A.7. As an example, we calculate the standard orientation of the diagram $(I_{k,l})_{\text{max}}$:

$$(I_{k,l})_{\text{max}} = \begin{array}{c} e_{k+l} \dots e_{k+1} \\ \text{---} \bullet \text{---} \\ e_1 \dots e_k \end{array}$$

where k leaves are attached at the top right and l leaves are attached at the bottom left, and we labeled the edges by e_1, \dots, e_{k+l} as shown. We claim that the standard orientation is:

$$\omega_{(I_{k,l})_{\text{max}}}^{\text{std}} = (-1)^l \cdot e_1 \wedge \cdots \wedge e_{k+l}$$

Proof. Starting from the orientation of the right diagram in Figure 7, we move the lower branch across the upper k leaves, with the following induced orientation:

$$\begin{array}{c} \text{---} \bullet \text{---} \\ e_1 \dots e_k \end{array} \begin{array}{c} e_{k+1} \\ \text{///} \end{array} \rightsquigarrow \dots \rightsquigarrow \begin{array}{c} \text{---} \bullet \text{---} \\ e_1 \dots e_k \end{array} \begin{array}{c} e_{k+1} \\ \text{///} \end{array}$$

$$e_1 \wedge \cdots \wedge e_{k+l} \qquad \qquad \qquad (-1)^k \cdot e_1 \wedge \cdots \wedge e_{k+l}$$

Moving the lower branch over the thick vertex, and relabeling the edges, we obtain the induced standard orientation:

$$\rightsquigarrow \begin{array}{c} \text{---} \bullet \text{---} \\ e_1 \dots e_k \end{array} \begin{array}{c} e_{k+1} \\ \text{///} \end{array} = \begin{array}{c} \text{---} \bullet \text{---} \\ e_1 \dots e_k \end{array} \begin{array}{c} e_{k+1} \\ \text{///} \end{array}$$

$$(-1)^{k+1} \cdot e_1 \wedge \cdots \wedge e_{k+l} \qquad \qquad \qquad (-1)^1 \cdot e_1 \wedge \cdots \wedge e_{k+l}$$

Finally, we move the edges e_{k+2}, \dots, e_{k+l} over to the thick left edge.

$$\begin{array}{ccc}
 \rightsquigarrow & \begin{array}{c} \text{Diagram 1: A thick horizontal line with a black dot. To the left, several thin horizontal lines labeled } e_{k+3}, \dots, e_{k+l} \text{ are connected to the thick line. To the right, thin lines labeled } e_{k+2}, e_{k+1} \text{ are connected to the dot. Further right, a thick line with four diagonal slashes is labeled } e_1 \dots e_k. \end{array} & \rightsquigarrow \dots \rightsquigarrow \\
 & (-1)^2 \cdot e_1 \wedge \dots \wedge e_{k+l} & \begin{array}{c} \text{Diagram 2: A thick horizontal line with a black dot. To the left, a thick line with four diagonal slashes is labeled } e_{k+l} \dots e_{k+1}. To the right, thin lines labeled } e_1 \dots e_k \text{ are connected to the dot. Further right, a thick line with four diagonal slashes is labeled } e_1 \dots e_k. \end{array} \\
 & & (-1)^l \cdot e_1 \wedge \dots \wedge e_{k+l}
 \end{array}$$

Thus, $\omega_{(I_{k,l})_{\max}}^{\text{std}} = (-1)^l \cdot e_1 \wedge \dots \wedge e_{k+l}$ is the standard orientation with edges labeled as described above. This completes the proof. \square

Our last task in this subsection is to define the orientation $\omega(S, D)$ that is needed in the definition of the morphism p for a generator $(D, f_\cup, m, \omega_D) \in Q_k \hat{\mathcal{A}}$ of degree k , and a diagram S with $S_{\max} \leq D_{\min}$. This will be done in four steps: First, we define the orientation ξ_B for binary diagrams B , second, we define the contraction $\omega \rfloor \xi_B$, third, we define notion of positive and negative edges and show how they are relevant for p , and fourth we use the notion of positive and negative edges to find the orientation $\omega(S, D)$ on S by contracting $\omega \rfloor \xi_{S_{\max}}$ for some ω .

Step 1. Following [MS], we first define the orientation

$$\xi_B := (-1)^{\frac{(n-2)(n-3)}{2}} \cdot \omega_B^{\text{std}} = (-1)^{1+2+\dots+(n-3)} \cdot \omega_B^{\text{std}}$$

for a binary diagram B with standard orientation ω_B^{std} , n leaves, and $n - 2$ edges.

Remark A.8. There is an alternative description of ξ_B given in [MS]. For this, first define $\xi_B = +1$ for the binary diagrams B in $C_0 \hat{\mathcal{A}}$ with 2 leaves and no edges (*i.e.* $B = T_2, M_{1,0}, M_{0,1}$, or $I_{0,0}$). Then for a general binary diagram B , the orientation ξ_B is determined by the composition relation in $C_0 \hat{\mathcal{A}}$,

$$(B' \circ_{f_\cup(i)} B'', f_\cup, \xi_{B' \circ_{f_\cup(i)} B''}) = \sigma \cdot ((B', f_\cup, \xi_{B'}) \circ_i (B'', f_\cup, \xi_{B''})).$$

We can derive this formula by comparing ξ_B for two binary diagrams related by one of the local moves from Definition A.3.

Step 2. If B is a binary tree with orientation ω , and ω' is an orientation on a subset of edges of B , then define $\omega' \rfloor \omega$ by the relation $\langle e', e \rangle = \delta_{e', e} \in \{0, 1\}$, where $\delta_{e', e}$ denotes the Kronecker delta. In particular, if $\omega = e_1 \wedge \dots \wedge e_r \wedge e_{r+1} \wedge \dots \wedge e_k$ and $\omega' = e_1 \wedge \dots \wedge e_r$, then

$$\omega' \rfloor \omega = (-1)^{\frac{r(r-1)}{2}} \cdot e_{r+1} \wedge \dots \wedge e_k.$$

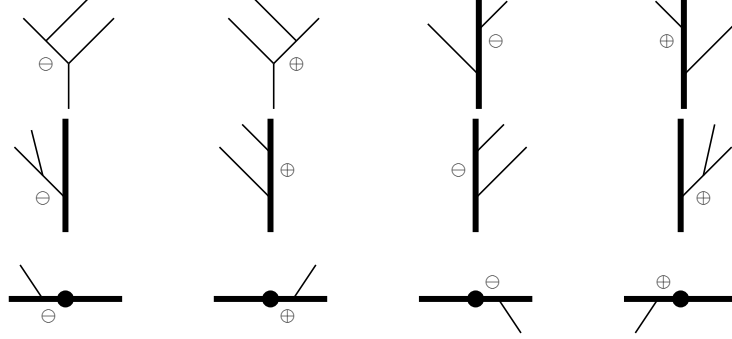
Now, if $S_{\max} = D_{\min}$, then as we shall see in Step 3, $S = D_{\min} / \{\text{edges in } D\}$, in which case we define $\omega(S, D) = \omega_D \rfloor \xi_{D_{\min}}$. Now, consider a corolla c for example. Since $1 \rfloor \omega = \omega$ and $\omega_B^{\text{std}} \rfloor \xi_B = +1$, we obtain

$$(A.5) \quad S = c_{\min}, D = c, \omega_D = 1 \Rightarrow \omega(S, D) = 1 \rfloor \xi_{c_{\min}} = \xi_{c_{\min}},$$

$$(A.6) \quad S = c, D = c_{\max}, \omega_D = \omega_{c_{\max}}^{\text{std}} \Rightarrow \omega(S, D) = \omega_{c_{\max}}^{\text{std}} \rfloor \xi_{c_{\max}} = +1.$$

Step 3. To further analyze the condition $S_{\max} \leq D_{\min}$ we need to introduce the notion of positive and negative edges in a binary diagram. Markl and Shnider ([MS]) refer to these notions as left-leaning and right-leaning, respectively.

Definition A.9. Let B be a binary diagram. We define an edge to be positive, denoted by \oplus , respectively negative, denoted by \ominus , if it appears in B in the following way,



We denote the number of positive edges in a binary diagram B by $|B|_{\oplus}$.

Lemma A.10. *Positive and negative edges have the following properties:*

- (1) If $B \leq B'$, then $|B|_{\oplus} \leq |B'|_{\oplus}$, i.e., $|\cdot|_{\oplus}$ preserves the order. The maximal (resp. minimal) binary diagram c_{\max} (resp. c_{\min}) of a corolla c given by Lemma 4.2 is the unique diagram all of whose edges are positive (resp. negative).
- (2) If S is a diagram, then $S = S_{\max}/\{e_1, \dots, e_r\}$ is a quotient in which only positive edges of S_{\max} are collapsed. If D is a diagram, then $D = D_{\min}/\{e_1, \dots, e_s\}$ is a quotient in which only negative edges of D_{\min} are collapsed.
- (3) Let $(D, f_{\odot}, m, \omega_D) \in Q_k \hat{\mathcal{A}}$. If $|D_{\min}|_{\oplus} \neq k$, then $p(D, f_{\odot}, m, \omega_D) = 0$. If $|D_{\min}|_{\oplus} = k$, then $D = D_{\min}/\{\text{negative edges}\}$, and if $(S, f, \omega) \in C_k \hat{\mathcal{A}}$ is a summand of $p(D, f_{\odot}, m, \omega_D)$, then S_{\max} has exactly k positive edges and $S = S_{\max}/\{\text{positive edges}\}$.

Proof.

- (1) This can be checked by direct inspection.
- (2) For a diagram S , we obtain S_{\max} by inserting positive edges at every non-binary vertex. For a diagram D , we obtain D_{\min} by inserting negative edges at every non-binary vertex.
- (3) Since D has k edges and D_{\min} is obtained from D by inserting only negative edges, D_{\min} has at most k positive edges. If $(S, f, \omega) \in C_k \hat{\mathcal{A}}$, then S_{\max} is obtained from S by inserting k positive edges; consequently S_{\max} has at least k positive edges. Since $S_{\max} \leq D_{\min}$, we have $k \leq |S_{\max}|_{\oplus} \leq |D_{\min}|_{\oplus} \leq k$. Therefore S_{\max} and D_{\min} must have exactly k positive edges. Furthermore, the k positive edges in D_{\min} are exactly the ones coming from D , and the k positive edges in S_{\max} are exactly the ones inserted in S . □

Step 4. Now, let $(D, f_{\odot}, m, \omega_D) \in Q_k \hat{\mathcal{A}}$ be a generator of degree k , and let S be a diagram with $S_{\max} \leq D_{\min}$. In order to define $\omega(S, D)$, we may assume by Lemma A.10 (3), that exactly k edges e_1, \dots, e_k of D_{\min} are positive, and these are the edges of D , i.e., $\omega_D = \eta \cdot e_1 \wedge \dots \wedge e_k$ for some $\eta \in \{+1, -1\}$.

We can now define $\omega(S, D)$ in the general case.

Definition A.11. If $S_{\max} = D_{\min}$, then $S = D_{\min}/\{e_1, \dots, e_k\}$, and we set $\omega(S, D) := \omega_D \rfloor \xi_{D_{\min}}$ as in step 2. If $S_{\max} < D_{\min}$, then $S = S_{\max}/\{\text{positive edges}\}$ by Lemma A.10 (3), and we set $\omega(S, D) := (\eta \cdot e_1 \wedge \dots \wedge e_k) \rfloor \xi_{S_{\max}}$, where the positive edges in D_{\min} and S_{\max} are identified using the local moves from Definition A.3. The ambiguity of identifying positive edges under paths is given (according to the Coherence Lemma A.5) by pentagons, hexagons and squares. Since the pentagons and hexagons change the number of positive edges, changing a path $\beta = (D_{\min}, \dots, S_{\max})$ to another path $\beta' = (D_{\min}, \dots, S_{\max})$ only consists of squares, for which the positive edges remain identified uniquely. (Note, that for a local move $B \rightsquigarrow B'$ from Definition A.3 with constant number of positive edges, the procedure of keeping track of the positive edge by renaming a positive edge e_\oplus by one negative edge e_\ominus gives $\dots \wedge e_\ominus \wedge \dots \wedge e_\oplus \wedge \dots = -\dots \wedge e_\oplus \wedge \dots \wedge e_\ominus \wedge \dots$, which is the induced orientation $\xi_{B'}$ on B' .)

A.3. Sign check for Proposition 3.2. We now give the remaining sign details for Proposition 3.2. More precisely, in the notation of the proof of Proposition 3.2, we will show that $(-1)^{i+1} \omega_B^{\hat{e}_i}$ equals $(-1)^{\epsilon_2} \omega_j$.

We calculate $(-1)^{\epsilon_2} \omega_j$ of the binary diagram B from the proof of Proposition 3.2 and compare it to $\omega_B^{\hat{e}_i}$. Recall that B is a composition of B' and B'' with standard orientations corresponding to c' and c'' with $(-1)^{\epsilon_1} \cdot \sigma \cdot ((c', f_\cup, 1) \circ_j (c'', f'_\cup, 1)) = (D', f''_\cup, e')$ and $D'/e' = c$. If the corolla c' has r leaves and the corolla c'' has s leaves, then the original corolla c has $k = r + s - 1$ leaves. Hence, from the definition of the composition in Equation (2.1), and of the S_k action, we see that $(-1)^{\epsilon_1} = \text{sgn}(\sigma) \cdot (-1)^{j \cdot (s+1) + r \cdot s}$. Furthermore, from the definition of the composition in $Q_* \hat{A}$, we have $\omega_j = \omega_{B'}^{\text{std}} \wedge \omega_{B''}^{\text{std}}$. The only other signs come from comparing ω_j to ω_B^{std} , and a possible application of σ . We consider two cases: Case 1: $\sigma = id_k$. Case 2: $\sigma \neq id_k$.

Case 1: Either the corolla c is *not* an inner product diagram, or c is an inner product diagram and the composition \circ_j is *not* on the thick left module input.

Case 2: The corolla c is an inner product diagram and the composition \circ_j is on the thick left module input.

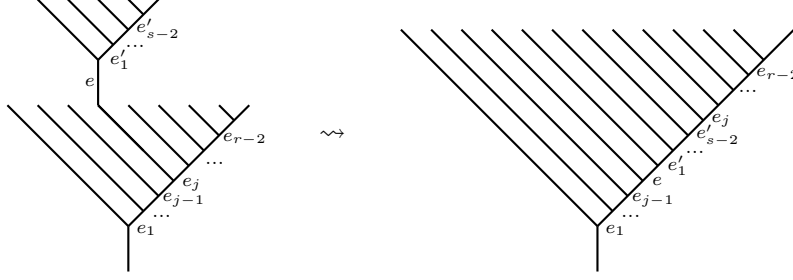
In Case 1, the only way to obtain $(c, f_\cup, 1)$ as a composition of c' and c'' is via the canonical labelings f_\cup for c' and c'' and $\sigma = id$. In this case, the proof follows as in [MS, Proposition 4.2]. More precisely, with the notation from the left diagram in Figure 8, we have

$$\begin{aligned} (-1)^{\epsilon_2} \omega_j &= (-1)^{j(s+1)+rs} \cdot e_1 \wedge \dots \wedge e_{r-2} \wedge e'_1 \wedge \dots \wedge e'_{s-2} \\ &= (-1)^{j+s} \cdot e_1 \wedge \dots \wedge e_{j-1} \wedge e'_1 \wedge \dots \wedge e'_{s-2} \wedge e_j \wedge \dots \wedge e_{r-2}. \end{aligned}$$

On the other hand, the standard orientation for the left diagram in Figure 8 is $\omega_B^{\text{std}} = (-1)^{s-1} \cdot e_1 \wedge \dots \wedge e_{j-1} \wedge e \wedge e'_1 \wedge \dots \wedge e'_{s-2} \wedge e_j \wedge \dots \wedge e_{r-2}$, which can be seen via the $(s-1)$ local moves to the diagram on the right in Figure 8. Setting $i = j$, we obtain,

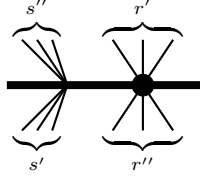
$$(-1)^{i+1} \omega_B^{\hat{e}_i} = (-1)^{j+s} \cdot e_1 \wedge \dots \wedge e_{j-1} \wedge e'_1 \wedge \dots \wedge e'_{s-2} \wedge e_j \wedge \dots \wedge e_{r-2} = (-1)^{\epsilon_2} \omega_j.$$

The considerations in other types of diagrams for Case 1 are similar to the one in Figure 8.

FIGURE 8. Move the edges e, e'_1, \dots, e'_{s-2} to the right.

Now, for Case 2, where $c' = I_{r', r''}$ is an inner product corolla and $c'' = M_{s', s''}$ is a module tree with $r = r' + r'' + 2$ and $s = s' + s'' + 1$, we have

$$(I_{r', r'', f_{\circlearrowleft}, 1) \circ_1 (M_{s', s'', f_{\circlearrowleft}, 1) = (-1)^{(s+1)+r \cdot s} \cdot (I_{r'+s'', r''+s'}, f_{\circlearrowleft} \circ \tau^{s'}, 1),$$



where $\tau \in \mathbb{Z}_k \subset S_k$ is the cyclic rotation “ $-1 \pmod k$ ”. Thus, $\sigma = \tau^{s'}$ with $\text{sgn}(\sigma) = (-1)^{s' \cdot (r+s')}$, and thus $(-1)^{\epsilon_1} = (-1)^{s+1+rs+s'(r+s')}$. Similarly we obtain (see Figure 9)

$$(-1)^{\epsilon_2} \omega_1 = (-1)^{s+1+rs+s'(r+s')} \cdot e_1 \wedge \dots \wedge e_{r-2} \wedge e'_1 \wedge \dots \wedge e'_{s-2}.$$

On the other hand, the standard orientation of the left diagram in Figure 9 is

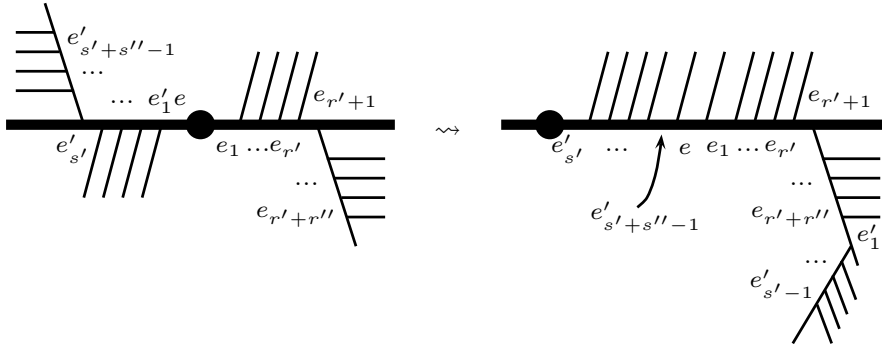


FIGURE 9. The edges on the left are brought to the right in $(s + r - 3)$ moves: $s' - 1$ to move $e'_1, \dots, e'_{s'}$ on one branch; 2 to move the obtained two main branches from left to right; $r' + r''$ to move the “ s'' ”-branch all the way to the right; and $s'' - 1$ to move the edges from the “ s'' ”-branch to the thick right edge.

$$\begin{aligned}\omega_B^{\text{std}} &= (-1)^{s-1+r} \cdot e'_{s'} \wedge \cdots \wedge e_{s'+s''-1} \wedge e \wedge e_1 \wedge \cdots \wedge e_{r-2} \wedge e'_1 \wedge \cdots \wedge e'_{s'-1} \\ &= (-1)^{s-1+r+s''(r+s')} \cdot e \wedge e_1 \wedge \cdots \wedge e_{r-2} \wedge e'_1 \wedge \cdots \wedge e'_{s'-1} \wedge e'_{s'} \wedge \cdots \wedge e'_{s-2},\end{aligned}$$

which can be seen by performing $(s+r-3)$ local moves yielding the right diagram in Figure 9. Thus for $i=1$, we obtain

$$(-1)^{i+1} \cdot \omega_B^{\hat{e}} = (-1)^{s+r-3+s''(r+s')} \cdot e_1 \wedge \cdots \wedge e_{r-2} \wedge e'_1 \wedge \cdots \wedge e'_{s-2} = (-1)^{\epsilon_2} \cdot \omega_1,$$

where we used the fact that $s = s' + s'' + 1$, so that $(-1)^{r+s''r} = (-1)^{rs+s'r}$.

This completes the check of both cases, and with this also the proof of Proposition 3.2.

APPENDIX B. PROOF OF PROPOSITION 3.3

In this appendix, we prove Proposition 3.3: *The cellular complexes associated with T_n , $M_{k,l}$, and $I_{k,l}$ are contractible.* The cellular complex associated with T_n is the associahedron K_n , whose contractibility was proved by J. Stasheff in [S, Proposition 3]. Since the cellular complexes associated with $M_{k,n-k}$, $I_{n,0}$ and $I_{0,n}$ are also isomorphic to K_n , our task is to verify the contractibility of the cellular complex $|I_{k,l}|$ associated with $I_{k,l}$ for each $k, l \geq 1$. To this end, we derive an analog of Stasheff's result, which shows that $|I_{k,l}|$ is homeomorphic to the (closed) $(k+l)$ -ball B^{k+l} .

We begin with an outline of the ideas involved. Fix natural numbers $k, l \geq 1$, and let $n = k + l$. First, we identify the boundary of $|I_{k,l}|$ with the union of two closed $(n-1)$ -balls glued together along their bounding $(n-2)$ -spheres. Roughly speaking, these ‘‘upper’’ and ‘‘lower’’ boundary components are obtained by inserting edges into the upper and the lower parts of $I_{k,l}$, respectively, *cf.* Definition B.2. Second, we identify this common $(n-2)$ -sphere with those diagrams obtained from $I_{k,l}$ by inserting at least one upper and one lower edge. Third, recalling that Stasheff represented the associahedron K_{n+2} as a subdivision of a cube [S, Section 6], we establish bijections between the upper and lower boundary components of $|I_{k,l}|$ and the interior of the union of the boundary components $\partial_2, \dots, \partial_{k+2}$ of K_{n+2} (see Figure 14 on page 29), which we denote by $|K_{n+2}^{\{2, \dots, k+2\}}|$.

Definition B.1. Label the leaves of $I_{k,l}$, K_{n+2} , and diagrams D in $\partial I_{k,l}$ or ∂K_{n+2} , using the canonical labeling f_\circ . Given such a diagram D and an edge e of D , let t be the smallest positive integer that labels a leaf outward from e , and assign the label t to e . If D is in $\partial I_{k,l}$ and $t \in \{2, \dots, k+2\}$, we say that e is an *upper edge* of D ; otherwise e is a *lower edge* of D . Likewise, a leaf of $I_{k,l}$ or D with label in $\{2, \dots, k+2\}$ is an *upper leaf*; otherwise it is a *lower leaf*.

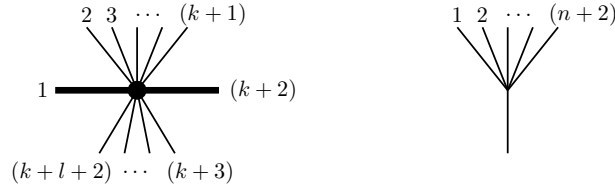


FIGURE 10. The canonical labeling of leaves

The leaves and edges of the diagrams in Figure 11, for example, are labeled as specified by Definition B.1; the upper edges and leaves of the left-hand diagram are labeled by elements of $\{2, \dots, 17\}$.

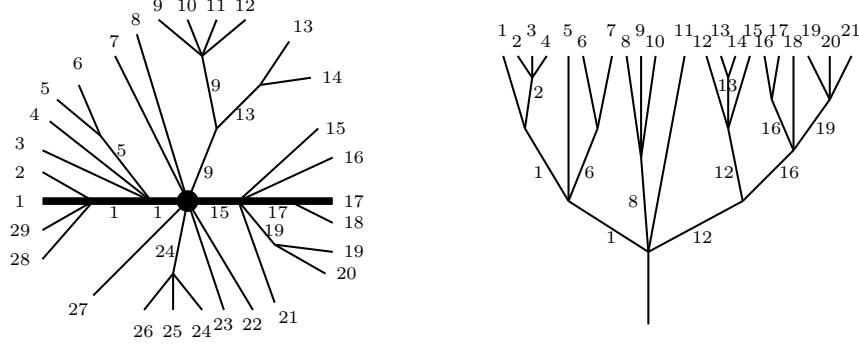
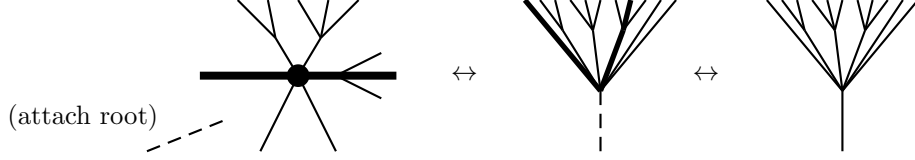


FIGURE 11. The labeling of the edges

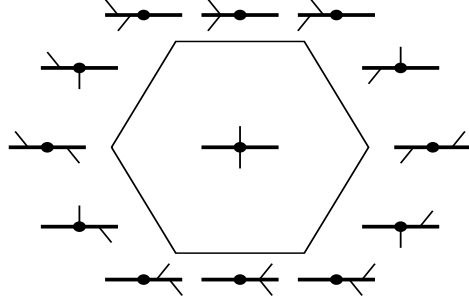
Since the label of an edge e in a labeled diagram D is determined by the labels of leaves outward from e , inserting an edge into D or contracting an edge of $D \setminus \{e\}$ preserves the label of e . In particular, the boundary operator ∂ , which is defined by summing over all possible ways of inserting an edge, preserves labels.

Definition B.2. Let $X \subset \{1, \dots, n+2\}$ and let $I_{k,l}^X$ (respectively K_{n+2}^X) denote the module generated by all diagrams in $\partial I_{k,l}$ (respectively ∂K_{n+2}) whose edges are labeled by elements of X . For example, the diagrams in Figure 11 lie in $I_{15,12}^{\{1,5,9,13,15,17,19,24\}}$ and $K_{21}^{\{1,2,6,8,12,13,16,19\}}$, respectively. Note that many edges may have the same label, and $I_{k,l}^X = 0$ for many subsets X . In particular, $I_{k,l}^+ := I_{k,l}^{\{2, \dots, k+2\}}$ is the module generated by all diagrams with *at least one upper edge but no lower edges*, and $I_{k,l}^- := I_{k,l}^{\{1, k+3, \dots, k+l+2\}}$ is the module generated by all diagrams with *at least one lower edge but no upper edges*. Generators of $I_{k,l}^+$ are called *upper diagrams*; generators of $I_{k,l}^-$ are called *lower diagrams*. Of course, $I_{k,l}^+ \cap I_{k,l}^- = \emptyset$. Furthermore, denote the module generated by diagrams with *at least one upper edge* by $\overline{I_{k,l}^+}$; denote the module generated by diagrams with *at least one lower edge* by $\overline{I_{k,l}^-}$. Then $I_{k,l}^+ \subset \overline{I_{k,l}^+}$ and $I_{k,l}^- \subset \overline{I_{k,l}^-}$, and in fact, the geometric realizations $|\overline{I_{k,l}^+}|$ and $|\overline{I_{k,l}^-}|$ are the respective closures of $|I_{k,l}^+|$ and $|I_{k,l}^-|$, *i.e.*, $|\overline{I_{k,l}^+}| = |\overline{I_{k,l}^+}|$ and $|\overline{I_{k,l}^-}| = |\overline{I_{k,l}^-}|$. Finally, $C_*(I_{k,l}) := \langle I_{k,l} \rangle \oplus \overline{I_{k,l}^+} \oplus \overline{I_{k,l}^-}$ is the module generated by $I_{k,l}$ and all diagrams obtained from $I_{k,l}$ by inserting edges.

There is the following important bijection $I_{k,l}^+ \leftrightarrow K_{k+l+2}^{\{2, \dots, k+2\}}$: Given an upper diagram D , produce the corresponding tree $T \in K_{k+l+2}^{\{2, \dots, k+2\}}$ by changing thick colors to thin and attaching a root between the first and last leaf (see Figure 12). Recover D from T by detaching the root and changing the color of the branches containing the first and $(k+2)^{\text{nd}}$ leaves from thin to thick. The tools we need to prove Proposition 3.3 are now in place.


 FIGURE 12. The correspondence $I_{k,l}^+ \leftrightarrow K_{k+l+2}^{\{2,\dots,k+2\}}$

Proof of Proposition 3.3. We wish to realize $C_*(I_{k,l})$ as a cellular complex $|I_{k,l}| \cong \bar{B}^{k+l}$, for each $k, l \geq 1$. First note that $|I_{1,1}| \cong \bar{B}^2$ (see Figure 13). Inductively,


 FIGURE 13. The hexagon induced by $I_{1,1}$

assume that $|I_{k',l'}| \cong \bar{B}^{k'+l'}$ for all $k' + l' < k + l$, and note that $\partial C_*(I_{k,l}) = I_{k,l}^+ \oplus I_{k,l}^- \oplus (\overline{I_{k,l}^+} \cap \overline{I_{k,l}^-})$, *i.e.*, all upper diagrams, lower diagrams, and diagrams with both upper and lower edges. The proof follows in three steps:

Step 1: $|I_{k,l}^+|$ and $|I_{k,l}^-|$ are homeomorphic to the open ball B^{k+l-1} .

Step 2: $|\overline{I_{k,l}^+}|$ and $|\overline{I_{k,l}^-}|$ are homeomorphic to the closed ball \bar{B}^{k+l-1} .

Step 3: $|\overline{I_{k,l}^+} \cap \overline{I_{k,l}^-}| \cong S^{k+l-2}$.

Steps 2 and 3 imply that $|\partial C_*(I_{k,l})|$ is homeomorphic to the union of two closed $(k+l-1)$ -balls glued together along their bounding $(k+l-2)$ -spheres. Thus $|I_{k,l}| \cong \bar{B}^{k+l}$ and the proof is complete. \square

Proof of step 1. In [S, Section 6], Stasheff gave an explicit realization of $K_{n+2}^{\{2,\dots,k+2\}}$ homeomorphic to an (open) ball B^{n-1} in ∂I^n . Since the correspondence $I_{k,l}^+ \leftrightarrow K_{n+2}^{\{2,\dots,k+2\}}$ preserves boundary, it defines a homeomorphism of geometric realizations. Thus $|I_{k,l}^+| \cong |K_{n+2}^{\{2,\dots,k+2\}}| \cong B^{n-1}$. The identification $I_{k,l}^- \leftrightarrow K_{n+2}^{\{2,\dots,l+2\}}$ is established by relabeling leaves: Assign “1” to the right-most leaf and continue clockwise, thereby replacing the original labels $k+3, \dots, k+l+2, 1$ with $2, \dots, l+2$, respectively; thus $|I_{k,l}^-| \cong |K_{n+2}^{\{2,\dots,k+2\}}|$ and the conclusion follows. \square

Proof of step 2. Lemma B.3 below asserts that the homeomorphisms of realizations $|I_{k,l}^+| \cong |I_{k,l}^-| \cong |K_{n+2}^{\{2,\dots,k+2\}}| \cong B^{n-1}$ extend to homeomorphisms of closures. Thus $|\overline{I_{k,l}^+}| \cong |\overline{I_{k,l}^-}| \cong |\overline{K_{n+2}^{\{2,\dots,k+1\}}}| \cong \bar{B}^{n-1}$. \square

Proof of step 3. Note that the sets $\partial\overline{I_{k,l}^+} = \overline{I_{k,l}^+} \setminus I_{k,l}^+$ and $\partial\overline{I_{k,l}^-} = \overline{I_{k,l}^-} \setminus I_{k,l}^-$ are identical and consist of all diagrams with at least one upper and one lower edge. Thus $|\overline{I_{k,l}^+} \cap \overline{I_{k,l}^-}| = |\partial\overline{I_{k,l}^+}| = \partial|\overline{I_{k,l}^+}| \cong S^{k+l-2}$. \square

Lemma B.3. *The homeomorphism of realizations $|I_{k,l}^+| \cong |K_{n+2}^{\{2,\dots,k+2\}}|$ defined above extends to a homeomorphism of closures $|\overline{I_{k,l}^+}| \cong |\overline{K_{n+2}^{\{2,\dots,k+1\}}}|$.*

Proof. In the proof of [S, Proposition 3], Stasheff showed how to construct a cellular homeomorphism $|K_{n+2}^{\{2,\dots,k+2\}}| \cong B^{n-1}$ and extend it to closures $|\overline{K_{n+2}^{\{2,\dots,k+2\}}}| \cong \bar{B}^{n-1}$. We wish to realize $|\overline{I_{k,l}^+}|$ in a similar way (see Figure 14). Given a diagram $D \in I_{k,l}^+$, let T be the corresponding tree under the isomorphism $I_{k,l}^+ \approx K_{n+2}^{\{2,\dots,k+2\}}$ established in step 1, and let α be the cell of B^{n-1} identified with T under Stasheff's identification. Then D is identified with α . Our goal is to extend this identification to $\overline{I_{k,l}^+} \leftrightarrow \bar{B}^{n-1}$.

Consider a cell $\alpha \subset B^{n-1}$ and the corresponding diagram $D \in I_{k,l}^+$. If $\bar{\alpha} \subset B^{n-1}$, the cells of $\bar{\alpha}$ have already been identified with generators of $I_{k,l}^+$. So assume that $\bar{\alpha} \cap \partial\bar{B}^{n-1} \neq \emptyset$. If $\dim \alpha = 1$, the 1-cell of α corresponds to an upper diagram $D \in I_{k,l}^+$, which differs from a binary diagram at exactly one vertex, which is either the root with valence 3 or another vertex of valence 4. Some edge insertion at this particular vertex produces a binary diagram $D' \in \overline{I_{k,l}^+}$ identified with an endpoint of $\bar{\alpha}$ in $\partial\bar{B}^{n-1}$.

Inductively, if $\alpha' \subset B^{n-1}$ is a cell of dimension less than r , assume that all cells in its closure $\bar{\alpha}'$ have been identified with diagrams in $\overline{I_{k,l}^+}$, and consider a diagram $D \in I_{k,l}^+$ whose corresponding cell $\alpha \subset B^{n-1}$ has dimension r and satisfies $\bar{\alpha} \cap \partial\bar{B}^{n-1} = \emptyset$. Since α also corresponds to a tree in $K_{n+2}^{\{2,\dots,k+2\}}$, we know that $\bar{\alpha} \cong \bar{B}^r$ and $\partial\bar{\alpha} \cap B^{n-1} \cong \bar{B}^{r-1}$. Using Stasheff's notation in [S, Sections 3 and 6], recall that $|K_{n+2}^{\{2,\dots,k+2\}}|$ is homeomorphic to the complement of the union of the closures of boundary components $\partial_j(s,t)(K_s \times K_t)$ over all $s+t = n+1$ with either $j = 1$ or $j > k+2$. Now if α corresponds to a product of cells $\partial_j(s,t)(K_s \times K_t)$, there is the corresponding identification with some product of diagrams $D' \times D''$, and Stasheff's decomposition of faces of associahedra as Cartesian products of associahedra identifies $D' \times D''$ with the corresponding diagram $D \in I_{k,l}^+$, the exact form of which is unimportant here. But what *is* important here is the fact that $|D| \cong B^r$. Furthermore, the cells in the boundary component $\partial\bar{\alpha} \cap B^{n-1}$ can be realized by a union of cells $\partial_j(s,t)(\partial K_s \times K_t)$ or $\partial_j(s,t)(K_s \times \partial K_t)$ whose union is a cellular complex homeomorphic to \bar{B}^{r-1} . By the induction hypothesis, there is a corresponding sum of products of diagrams, which corresponds to a sum of diagrams in $\overline{I_{k,l}^+}$ such that $\partial\bar{\alpha} \cap B^{n-1} \cong \bar{B}^{r-1}$. Thus the cellular structure of α extends to

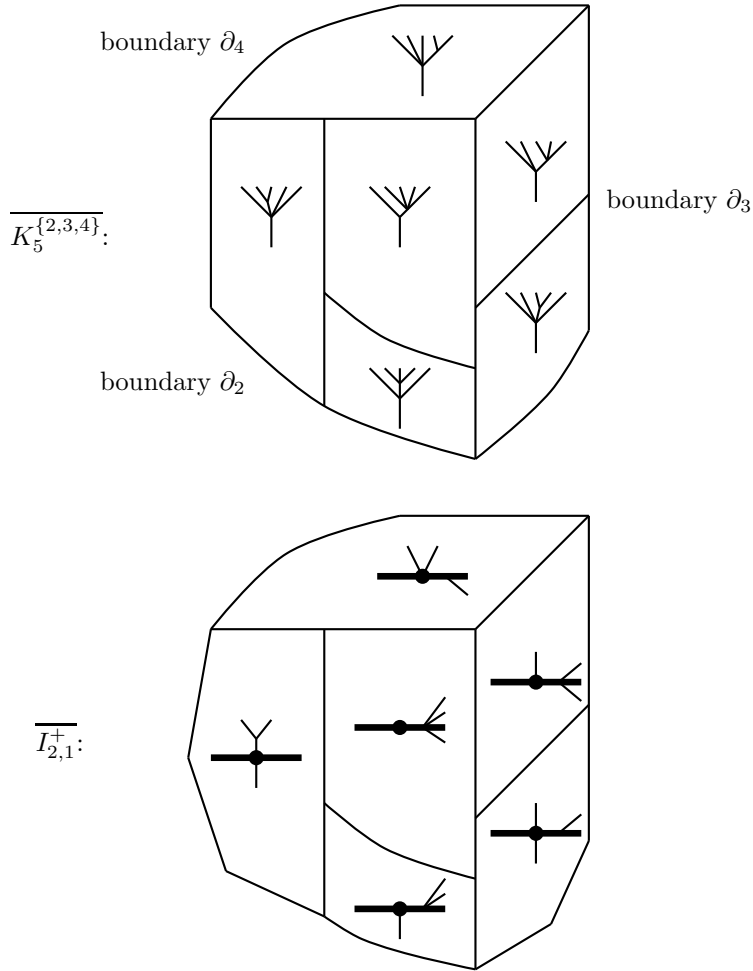


FIGURE 14. Identification between $I_{2,1}^+$ and $K_5^{\{2,3,4\}}$ (see also [S, Figure 18])

all of $\bar{\alpha}$ in such a way that the cells of $\partial\bar{\alpha}$ are realizations of the diagrams in $\overline{I_{k,l}^+}$ obtained by inserting edges into D in all possible ways.

Furthermore there is a bijective correspondence between cells of $\overline{I_{k,l}^+}$ and those in \bar{B}^{n-1} , which realize $\overline{I_{k,l}^+}$ as a closed $(n-1)$ -ball. To see this, note that the assignment of diagrams from $\overline{I_{k,l}^+}$ to cells of \bar{B}^{n-1} is surjective by construction, and respects the boundary, since it does so locally for each closed cell. We also claim that two diagrams D_1 and D_2 that correspond to the same cell in \bar{B}^{n-1} must be equal. First, this is clear for $\alpha \subset B^{n-1}$. To see this for $\alpha \subset \partial\bar{B}^{n-1}$, assume α corresponds to D_1 and D_2 . Then α is in the boundary of a unique smallest dimensional cell α' in the interior of B^{n-1} . Denote by D' the diagram corresponding to α' . Now, D_1 itself is in the boundary of some diagram D'' in $I_{k,l}^+$, and we denote by α'' the cell corresponding to D'' . Since D_1 is in the boundary of D'' , α must be in the

boundary of α'' . Since α' is the lowest dimensional cell containing α , α' must be in the boundary of α'' or equal to it. Since B^{n-1} realizes $I_{k,l}^+$, it must also be that D' is in the boundary of D'' or equal to it. In any case, since D'' is realized by α'' , we see that D_1 is in the boundary of D' . A similar argument shows that D_2 is also in the boundary of D' . Again, using that D' is realized by α' , we see that there is only one diagram $D_1 = D_2$ corresponding to the cell α . Therefore $\overline{I_{k,l}^+}$ is realized by a cell decomposition of \overline{B}^{n-1} .

This completes the proof of the lemma. \square

APPENDIX C. PROOF THAT “ \leq ” IS A PARTIAL ORDER

In this appendix, we show that the relation defined Definition 4.1 induces a well-defined partial ordering on binary diagrams. For diagrams $C_*\hat{\mathcal{A}}_y^{\mathbf{x}}$ with a coloring $\mathbf{x} = (1, \dots, 1)$, $y = 1$, this is a well-known fact known as the Tamari partial order, see [Ta]. We will extend this to binary diagrams in $C_*\hat{\mathcal{A}}$ of all colors.

It is sufficient to prove antisymmetry: $D = D'$ whenever $D \leq D'$ and $D' \leq D$. For a module diagram $D \in C_*\hat{\mathcal{A}}_y^{\mathbf{x}}$ of coloring $\mathbf{x} = (1, \dots, 2, \dots, 1)$, $y = 2$ let $\ell(D)$ (respectively $r(D)$) be the number of edges attached to the thick vertical edge coming from the left (respectively from the right), see Figure 15. Note that ℓ and

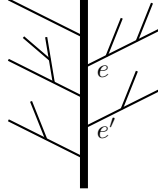


FIGURE 15. An example with $\ell(D) = 3$, $r(D) = 2$, $u(e) = 1$, $u(e') = 2$, $u(D) = 1 + 2 = 3$

r respect the order in the sense, if $D \leq D'$ then $\ell(D) \leq \ell(D')$ and $r(D) \geq r(D')$. Now, consider an edge e of D that is attached to the thick vertical edge from the right, and let $u(e)$ denote the number of edges that are attached to the thick edge from the left and that lie above e . Define $u(D) = \sum_e u(e)$, where the sum is taken over all edges e that are attached to the thick edge from the right (see Figure 15). Note, that relation (1) from Definition 4.1 leaves u invariant, whereas (2) preserves the order, *i.e.*, if $D < D'$ via the relation (2) then $u(D) < u(D')$.

Now, let $D, D' \in C_*\hat{\mathcal{A}}_y^{\mathbf{x}}$ with $\mathbf{x} = (1, \dots, 2, \dots, 1)$, $y = 2$. If $D \leq D'$ and $D' \leq D$ then we have $\ell(D) = \ell(D')$ and $r(D) = r(D')$. Since relation (3) strictly increases ℓ and relation (4) strictly decreases r , only relations (1) and (2) can be applied to generate $D \leq D'$ and $D' \leq D$. Furthermore, since (2) strictly increases u , we obtain that $u(D) = u(D')$, and only relation (1) can be applied. Using the known fact that (1) is a partial order implies the claim $D = D'$ for module diagrams $D, D' \in C_*\hat{\mathcal{A}}_y^{\mathbf{x}}$.

Finally, for inner product diagrams $D \in C_*\hat{\mathcal{A}}_y^{\mathbf{x}}$ with $\mathbf{x} = (1, \dots, 2, \dots, 2, \dots, 1)$, $y = 0$, let $t\ell(D)$ (resp. $bl(D)$, $tr(D)$, $br(D)$) be the number of edges attached to the top of the thick horizontal edge and left of the thick vertex (resp. bottom left, top right, and bottom right), see Figure 16. For $D \leq D'$, we have that $t\ell(D) \geq t\ell(D')$, $bl(D) \leq bl(D')$, $tr(D) \leq tr(D')$, and $br(D) \geq br(D')$. Thus, for

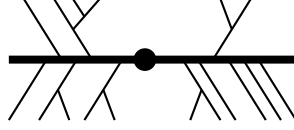


FIGURE 16. An example with $tl(D) = 2$, $bl(D) = 3$, $tr(D) = 1$, and $br(D) = 5$

$D \leq D'$ and $D' \leq D$, all of tl , bl , tr , and br coincide on D and D' . Since relations (3)-(6) change at least one of tl , bl , tr , or br , these cannot be applied to generate $D \leq D'$ and $D' \leq D$. To finish the proof, we refer back to the case of the module diagram with $\mathbf{x} = (1, \dots, 2, \dots, 1)$, $y = 2$, using the function u and the Tamari partial ordering as before to see that $D = D'$.

APPENDIX D. PROOF OF PROPOSITION 4.6 (p IS A CHAIN MAP)

In this appendix, we proof that $p : Q_*\hat{\mathcal{A}} \rightarrow C_*\hat{\mathcal{A}}$ is a chain map. The proof is an extension of Markl and Shnider's proof of Proposition 4.6 in [MS] and uses the notion of positive or negative edges in a binary inner product diagram as defined in Definition A.9 in Appendix A.2. The maximal binary diagrams is the one with only positive edges, and the minimal binary diagram is the one with only negative edges. (In [MS] these edges were called left and of right leaning edges, respectively.) The main part of the proof amounts to checking that for $(D, f_\circ, m, \omega_D) \in Q_k\hat{\mathcal{A}}$ such that D_{\min} has either k or $(k - 1)$ positive edges, $\partial_C \circ p(D, f_\circ, m, \omega_D) = p \circ \partial_Q(D, f_\circ, m, \omega_D)$. The case of $(k - 1)$ positive edges will be checked in Lemma D.1, and the case of k positive edges will be checked by induction beginning the induction in Lemma D.2.

Proof of Proposition 4.6. Since ∂_C and ∂_Q are derivations and p is multiplicative with respect to the composition \circ_i , it is enough to show that $\partial_C \circ p = p \circ \partial_Q$ on fully metric diagrams in $D \in Q_*\hat{\mathcal{A}}$. We do this by induction on the number of leaves $n = \mathcal{L}(D)$. For $n = 2$, it is trivial to check that $p : Q_*\hat{\mathcal{A}} \rightarrow C_*\hat{\mathcal{A}}$ is a chain map, since in this case $\partial_Q = 0$ and $\partial_C = 0$. We now assume that $p : Q_*\hat{\mathcal{A}} \rightarrow C_*\hat{\mathcal{A}}$ is a chain map when applied to any diagram with $\mathcal{L}(D) < n$ leaves, or compositions of diagrams with $\mathcal{L}(D) < n$ leaves. We need to show the same is true for metric diagrams with $\mathcal{L}(D) = n$ leaves.

For $(D, f_\circ, m, \omega_D) \in Q_k\hat{\mathcal{A}}$ with $n = \mathcal{L}(D)$ leaves, we have by Lemma A.10(3), that $p(D, f_\circ, m, \omega_D) = 0$ when $|D_{\min}|_\oplus \neq k$. Furthermore, if $\partial_Q(D, f_\circ, m, \omega_D) = \sum_i (D_i, \dots)$ and $|(D_i)_{\min}|_\oplus \neq k - 1$ then $p(D_i, \dots) = 0$. Since ∂_Q either preserves $|\cdot|_\oplus$ or decreases it by one, we see that $|(D_i)_{\min}|_\oplus$ either equals $|D_{\min}|_\oplus$ or $|D_{\min}|_\oplus - 1$. Thus, $p(\partial_Q(D, f_\circ, m, \omega_D)) = 0$ when $|D_{\min}|_\oplus \notin \{k, k - 1\}$. In particular for $|D_{\min}|_\oplus \notin \{k, k - 1\}$, we have $p(\partial_Q(D, f_\circ, m, \omega_D)) = 0 = \partial_C(p(D, f_\circ, m, \omega_D))$. In the case of $|D_{\min}|_\oplus = k - 1$, $p(\partial_Q(D, f_\circ, m, \omega_D)) = \partial_C(p(D, f_\circ, m, \omega_D))$ is the statement of Lemma D.1 below.

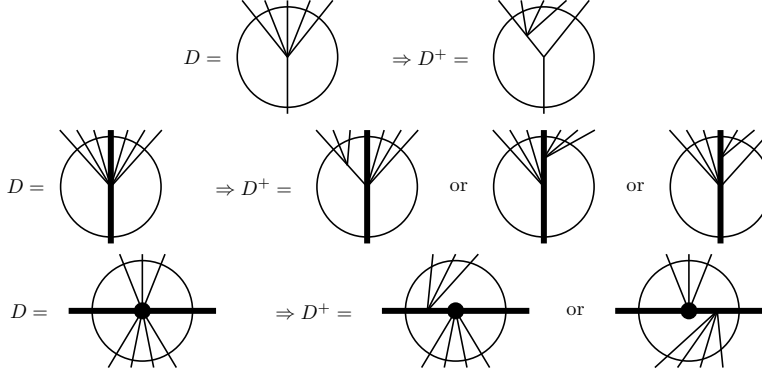
It remains to check the case $|D_{\min}|_\oplus = k$. The proof is a second induction on k starting from $k = n$. If $(B, f_\circ, m, \omega_B) \in Q_n\hat{\mathcal{A}}$ is a binary diagram with $|B|_\oplus = n$, then B is the maximal binary diagram, and $p(\partial_Q(B, f_\circ, m, \omega_B)) = \partial_C(p(B, f_\circ, m, \omega_B))$ is checked in Lemma D.2 below. Thus, we may now assume

$p(\partial_Q(D, f_\circ, m, \omega_D)) = \partial_C(p(D, f_\circ, m, \omega_D))$ for all $(D, f_\circ, m, \omega_D) \in Q_*\hat{\mathcal{A}}$ with either

- $\mathcal{L}(D) < n$ leaves, or compositions thereof,
- $\mathcal{L}(D) = n$ and $(D, f_\circ, m, \omega_D) \in Q_k\hat{\mathcal{A}}$ but $|D_{\min}|_\oplus \neq k$, or
- $\mathcal{L}(D) = n$ and $(D, f_\circ, m, \omega_D) \in Q_l\hat{\mathcal{A}}$ with $k < l \leq n$.

We wish to prove $p(\partial_Q(D, f_\circ, m, \omega_D)) = \partial_C(p(D, f_\circ, m, \omega_D))$ for $(D, f_\circ, m, \omega_D) \in Q_k\hat{\mathcal{A}}$ with $n = \mathcal{L}(D)$ leaves and $|D_{\min}|_\oplus = k$ (i.e. all k edges in D are inserted as positive edges).

Since D is non-binary, there exists a ternary (or higher) vertex v of D . Following [MS], we denote by D^+ the diagram given by inserting v in D in such a way that D_{\min}^+ has an extra negative edge e_v . This insertion is always possible. One approach is to use the following scheme:



Here, the diagram may be completed outside the circle in an arbitrary way, and the choice of D^+ may be determined by the number of incoming edges of a certain type.

We label the new edge e_v as metric, so that we calculate $\partial_Q(D^+, f_\circ, m, \omega) = \sum_e (D_e^+, \dots) + \sum_{e \neq e_v} (D^+/e, \dots) + (D^+/e_v, \dots)$, where D_e^+ is obtained by making the edge e non-metric, D^+/e is obtained by collapsing the edge e , and $D^+/e_v = D$. Note, that D_e^+ has a non-metric edge and is thus a composition of diagrams with fewer than n leaves, $(D^+/e, \dots) \in Q_k\hat{\mathcal{A}}$ with $|(D^+/e)_{\min}|_\oplus = k - 1$, and $(D^+, \dots) \in Q_{k+1}\hat{\mathcal{A}}$ all satisfy the chain condition $\partial_C p = p\partial_Q$ by the above hypothesis. Furthermore, (D^+, \dots) satisfying the chain condition implies the same for $\partial_Q(D^+, \dots)$, since $\partial_C p\partial_Q(D^+, \dots) = \partial_C \partial_C p(D^+, \dots) = 0 = p\partial_Q \partial_Q(D^+, \dots)$. Thus, $(D, \dots) = \partial_Q(D^+, \dots) - \sum_e (D_e^+, \dots) - \sum_{e \neq e_v} (D^+/e, \dots)$ also satisfies the chain condition. This completes the inductive step. \square

Lemma D.1. *Let $(D, f_\circ, m, \omega_D) \in Q_k\hat{\mathcal{A}}$ be a fully metric diagram (D has k metric edges) with $|D_{\min}|_\oplus = k - 1$. Then*

$$p(\partial_Q(D, f_\circ, m, \omega_D)) = 0 = \partial_C(p(D, f_\circ, m, \omega_D)).$$

Proof. Lemma A.10(3) implies that $\partial_C(p(D, f_\circ, m, \omega_D)) = 0$; it is sufficient to show that $p(\partial_Q(D, f_\circ, m, \omega_D)) = 0$. Recall that D_{\min} is given by inserting negative edges in D . Consequently, the positive edges in D_{\min} do not come from inserting edges into D . Let e_1, \dots, e_{k-1} be the edges of D that become positive edges in D_{\min} , and let e_0 be the edge of D that becomes a negative edge in D_{\min} . Direct inspection shows that an inserted edge e_0 in D_{\min} can be negative in six possible ways. Figure

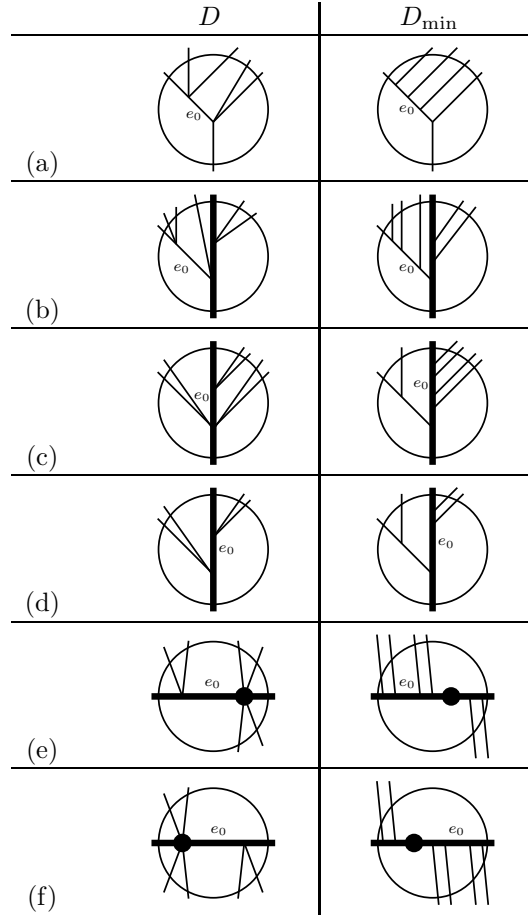


FIGURE 17. Here are the six ways for an edge to be inserted as a negative edge when considering D_{\min} .

17 shows the “local” pictures for these cases and their minima, where “local” means within a bigger diagram.

Recall from Definition 2.4 that $\partial_Q(D, f_\cup, m, \omega_D) \in Q_{k-1}\hat{\mathcal{A}}$ is given by a sum of diagrams $\sum_{i=0}^{k-1} D/e_i + \sum_{i=0}^{k-1} D_{e_i}$, where D/e_i is given by collapsing e_i , and D_{e_i} is given by relabeling e_i non-metric. Note that for $i > 0$, T_{e_i} is a composition of two diagrams along e_i . Consequently one of these two diagrams contains e_0 , giving a negative edge in its minimum, so that $p(D_{e_i}, \dots) = 0$ by Lemma A.10. Similarly, for those edges e_i such that D/e_i has less than $k - 1$ positive edges, we have $p(D/e_i, \dots) = 0$ by Lemma A.10. However, this only happens in restricted cases. First, $(D/e_0)_{\min} = D_{\min}$ so that $|(D/e_0)_{\min}|_{\oplus} = k - 1$, and additionally, in certain cases discussed below, it is possible that there is one more edge, denoted by e' , such that e_0 is converted to a positive edge when considering $(D/e')_{\min}$. Figure 18 illustrates this situation. To summarize, $p(D/e_i, \dots) = 0$ for all $e_i \notin \{e_0, e'\}$,

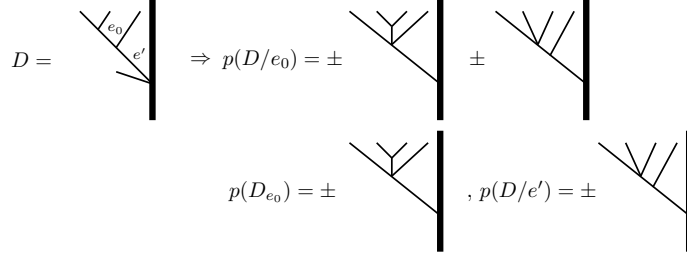


FIGURE 18. In the diagram D with edges e_0 and e' as above, we have $p(D/e_0, \dots) = \pm p(D_{e_0}, \dots) \pm p(D/e', \dots)$ and $p(D/e', \dots) = 0$.

and the check for $p(\partial_Q(D, f_\circlearrowleft, m, \omega_D)) = 0$ reduces to two cases:

$$\begin{cases} \text{Case 1: } p(D/e_0, \dots) = p(D_{e_0}, \dots) & , \text{ when } D \text{ has no edge } e', \\ \text{Case 2: } p(D/e_0, \dots) = p(D_{e_0}, \dots) \pm p(D/e', \dots) & , \text{ when } D \text{ has an edge } e'. \end{cases}$$

Case 1: The diagrams in Figure 19 depict the situations in which this case can occur. The proof that $p(D/e_0, \dots) = p(D_{e_0}, \dots)$ now follows. Since e_0 in D_{e_0} is non-metric, D_{e_0} decomposes as

$$(D_{e_0}, f_\circlearrowleft, m_{e_0}, \omega' \wedge \omega'') = \sigma \cdot ((D', f_\circlearrowleft, m, \omega') \circ_{e_0} (D'', f_\circlearrowleft, m, \omega'')),$$

so that

$$\begin{aligned} p(D_{e_0}, f_\circlearrowleft, m_{e_0}, \omega' \wedge \omega'') &= \sigma \cdot (p(D', f_\circlearrowleft, m, \omega') \circ_{e_0} p(D'', f_\circlearrowleft, m, \omega'')) \\ &= \sum_{S', S''} \sigma \cdot ((S', f_\circlearrowleft, \omega(S', D')) \circ_{e_0} (S'', f_\circlearrowleft, \omega(S'', D''))), \end{aligned}$$

where we sum over all S' and S'' with $S'_{\max} \leq D'_{\min}$ and $S''_{\max} \leq D''_{\min}$. On the other hand,

$$p(D/e_0, f_\circlearrowleft, m, \omega' \wedge \omega'') = \sum (S, f_\circlearrowleft, \omega(S, D)),$$

where we sum over all S with $S_{\max} \leq (D/e_0)_{\min} = D_{\min}$. Consequently, the equality $p(D/e_0, \dots) = p(D_{e_0}, \dots)$ follows (up to sign) by noting that each S_{\max} with $S_{\max} \leq D_{\min}$ is given by a composition along e_0 , *i.e.*, $S_{\max} = S'_{\max} \circ_{e_0} S''_{\max}$ (since, by the order relations, a change of e_0 when reducing D_{\min} also changes the number of positive edges). The proof of this case will be complete, once we compare the signs for $S' \circ_{e_0} S''$ and S . To calculate these signs, we assume that D' has r leaves and degree p with $\omega' = e'_1 \wedge \dots \wedge e'_p$, and D'' has s leaves and degree q with $\omega'' = e''_1 \wedge \dots \wedge e''_q$. Let $\xi_{D_{\min}}$, $\xi_{D'_{\min}}$ and $\xi_{D''_{\min}}$ denote the orientations from Step 1 in Appendix A.2. We first assume that $S_{\max} = D_{\min}$; then $S'_{\max} = D'_{\min}$ and $S''_{\max} = D''_{\min}$, and $\omega(S, D) = (\omega' \wedge \omega'') \rfloor \xi_{D_{\min}}$, $\omega(S', D') = \omega' \rfloor \xi_{D'_{\min}}$, and $\omega(S'', D'') = \omega'' \rfloor \xi_{D''_{\min}}$. We need to consider the cases $\sigma = id$ or $\sigma \neq id$; the latter occurs when S' is an inner product diagram and e_0 is a thick module edge on the left of S' .

- Let $\sigma = id$; then either S' is not an inner product diagram or \circ_{e_0} is not a composition at the first position. Assume e_0 composes at the i^{th} position. Then,

$$(S', f_\circlearrowleft, \omega(S', D')) \circ_i (S'', f_\circlearrowleft, \omega(S'', D''))$$

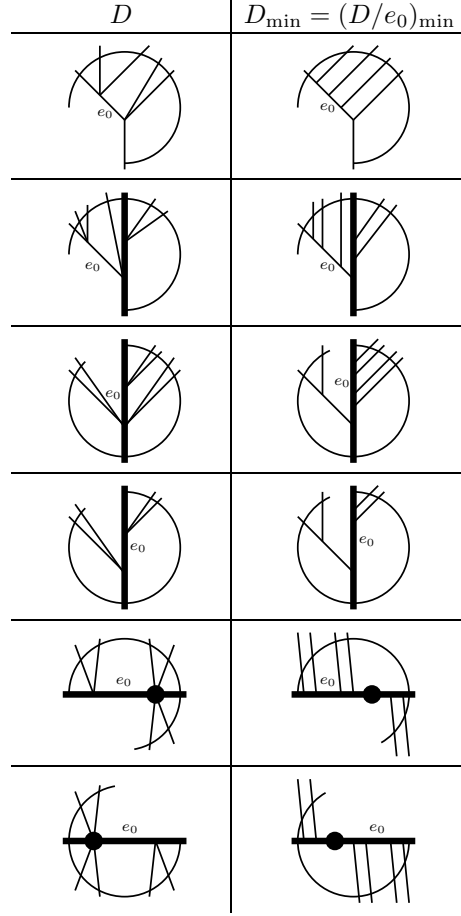


FIGURE 19. Case 1: p is non-vanishing only for D/e_0 and D_{e_0} . The open “half-circles” for D indicate that each diagram D may be completed in an arbitrary way outside the half-circle. Thus, a half-circle that connects to an edge denotes that more edges may be added on the side of the edge outside the half-circle.

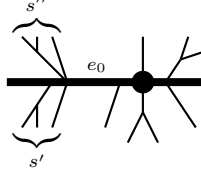
$$= (-1)^{i(s+1)+r \cdot q} (S' \circ_{e_0} S'', f_{\circlearrowleft}, (\omega'] \xi_{D'_{\min}}) \wedge (\omega''] \xi_{D''_{\min}}) \wedge e_0).$$

On the other hand, since $D_{\min} = D'_{\min} \circ_{e_0} D''_{\min}$, Remark A.8 shows that $\xi_{D_{\min}}$ is given by the canonically induced orientation coming from composing D'_{\min} and D''_{\min} with orientations $\xi_{D'_{\min}}$ and $\xi_{D''_{\min}}$, respectively. According to Equation (2.1) the induced orientation of this composition with sign given by $\epsilon = i(s+1) + r \cdot 0$ is:

$$\xi_{D_{\min}} = (-1)^{i(s+1)+r \cdot 0} \cdot \xi_{D'_{\min}} \wedge \xi_{D''_{\min}} \wedge e_0.$$

Therefore,

$$\begin{aligned} \omega(S, D) &= (\omega' \wedge \omega'')] \xi_{D_{\min}} = (-1)^{i(s+1)} (\omega' \wedge \omega'')] (\xi_{D'_{\min}} \wedge \xi_{D''_{\min}} \wedge e_0) \\ &= (-1)^{i(s+1)+r \cdot q} (\omega'] \xi_{D'_{\min}}) \wedge (\omega''] \xi_{D''_{\min}}) \wedge e_0. \end{aligned}$$

FIGURE 20. The composition $S' \circ_{e_0} S''$.

- Let $\sigma \neq id$; so that S' is an inner product diagram and the composition at e_0 is at the first position of S' . Assume that S'' is a module diagram with s' leaves to the left of the module branch, s'' leaves to the right of the module branch, and $s = s' + s'' + 1$; see Figure 20. Then as before, we obtain a sign of $(-1)^{1 \cdot (s+1) + r \cdot q}$ for the composition $S' \circ_{e_0} S''$ with orientation $(\omega'] \xi_{D'_{\min}}) \wedge (\omega''] \xi_{D''_{\min}}) \wedge e_0$, but the cyclic permutation introduces an additional sign of $(-1)^{s'(s''+r)}$. On the other hand, we may use Remark A.8 to calculate $\xi_{D_{\min}}$, which is again given by the orientations $\xi_{D'_{\min}}$ and $\xi_{D''_{\min}}$ and the fact that D_{\min} is given by the composition $D_{\min} = D'_{\min} \circ_{e_0} D''_{\min}$, now with an additional cyclic permutation σ . The sign for the composition $D_{\min} = D'_{\min} \circ_{e_0} D''_{\min}$ from Equation (2.1) is given by $\epsilon = 1 \cdot (s+1) + r \cdot 0$, and the sign coming from the permutation σ is $(-1)^{s'(s''+r)}$. This gives a total orientation $\xi_{D_{\min}}$ of

$$\xi_{D_{\min}} = (-1)^{s'(s''+r)} \cdot (-1)^{1 \cdot (s+1) + r \cdot 0} \cdot \xi_{D'_{\min}} \wedge \xi_{D''_{\min}} \wedge e_0.$$

Thus we obtain again the same sign as before:

$$\begin{aligned} \omega(S, D) &= (\omega' \wedge \omega'')] \xi_{D_{\min}} \\ &= (-1)^{s+1+s'(s''+r)} (\omega' \wedge \omega'')] (\xi_{D'_{\min}} \wedge \xi_{D''_{\min}} \wedge e_0) \\ &= (-1)^{1+s+r \cdot q + s'(s''+r)} (\omega'] \xi_{D'_{\min}}) \wedge (\omega''] \xi_{D''_{\min}}) \wedge e_0. \end{aligned}$$

For the general case $S_{\max} < D_{\min}$, note that any steps given by a local move that changes $\omega(S, D)$ correspond exactly to a local move that change $\omega(S', D')$ or $\omega(S'', D'')$ by the same sign.

Case 2: Considering those diagrams depicted in Figure 17 such that e_0 is the only negative edge, Figure 21 shows the situations in which Case 2 occurs. (Here, the cases that are symmetric with respect to a 180° symmetry, such as cases (e) and (f) in Figure 17, have been excluded.) As in Case 1 above, $p(D/e_0, \dots) = \sum_{S_{\max} \leq D_{\min}} (S, \dots)$. This sum contains all the terms that appear in

$$\begin{aligned} p(D/e_0, \dots) &= p(D' \circ_{e_0} D'', \dots) = \sigma \cdot p(D', \dots) \circ_{e_0} p(D'', \dots) \\ &= \sum_{S'_{\max} \leq D'_{\min}, S''_{\max} \leq D''_{\min}} (S', \dots) \circ_{e_0} (S'', \dots), \end{aligned}$$

where the signs can be checked as in Case 1. However, $p(D/e_0, \dots)$ can now have more terms. In fact, a direct inspection shows that the binary diagrams $S_{\max} \leq (D/e_0)_{\min}$ from Figure 21 are of two types: (1) those with terms using no local moves from Definition A.3 for e_0 , and (2) those with terms that use local moves. The first type is given by $p(D/e_0, \dots)$; the second type is given by $p(D/e', \dots)$.

It only remains to check that the induced signs for $p(D/e_0, \dots)$ and $p(D/e', \dots)$ cancel. We first assume that $S_{\max} = (D/e')_{\min}$. Denote the orientation for D by

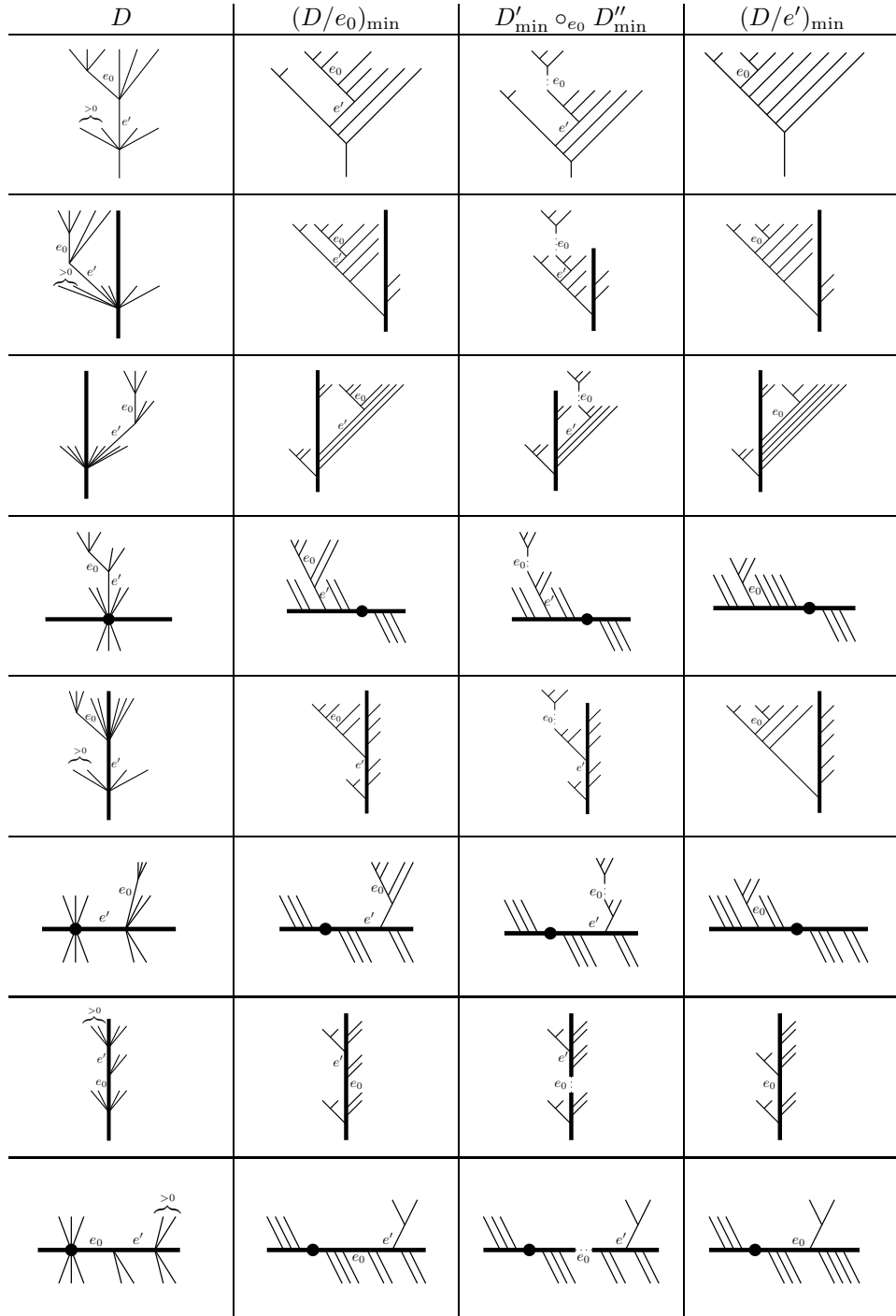


FIGURE 21. Case 2: p is non-vanishing for D/e_0 , D_{e_0} , and D/e' . Each of these diagrams may be completed in an arbitrary way. (To improve readability, the circle that were drawn in the previous diagrams have been omitted here.)

$\omega_D = \omega_R \wedge e_0 \wedge e'$, where ω_R stands for the orientation of the remaining edges in D . With this, the two terms D/e_0 and D/e' appear with opposite signs,

$$\partial_Q(D, f_\cup, m, \omega_D) = \pm \left((D/e_0, f_\cup, m, \omega_{D/e_0}) - (D/e', f_\cup, m, \omega_{D/e'}) \right) + \dots,$$

where $\omega_{D/e_0} = \omega_R \wedge e'$ and $\omega_{D/e'} = \omega_R \wedge e_0$. We claim that $p(D/e_0, f_\cup, m, \omega_{D/e_0}) = p(D/e', f_\cup, m, \omega_{D/e'})$. By assumption $S_{\max} = (D/e')_{\min}$; let us calculate the induced orientations $\omega(S, D/e_0)$ and $\omega(S, D/e')$ and show they coincide.

Note, that in each of the cases from Figure 21, there is a unique path of local moves from $(D/e_0)_{\min} = D_{\min}$ to $(D/e')_{\min}$ that preserves the number of positive edges. This path is determined by a sequence of edges e_1, \dots, e_j to which we apply the local moves. For example, in the first row in Figure 21, this sequence is depicted as e_1, e_2 on the left of Figure 22. Now, write $\xi_{D_{\min}}$ in the form $\xi_{D_{\min}} = e' \wedge e_1 \wedge \dots \wedge e_j \wedge e_0 \wedge \xi_R$

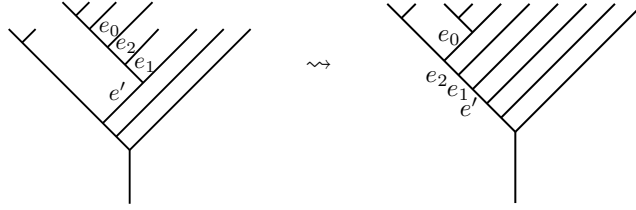


FIGURE 22. Local moves change $(D/e_0)_{\min}$ to $(D/e')_{\min}$.

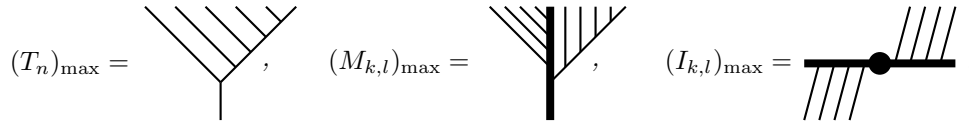
where ξ_R is the orientation on the remaining edges. In order to calculate $\omega(S, D/e_0)$ we need to perform a sequence of moves on e', e_1, \dots, e_j as depicted in Figure 22. At the i^{th} local move, the i^{th} orientation ξ_i changes by a factor of -1 , so that $\xi_i = (-1)^i \cdot e' \wedge e_1 \wedge \dots \wedge e_j \wedge e_0 \wedge \xi_R$. Keeping track of the positive edge, while making local moves, tells us that e_i is positive after the i^{th} move. After $j+1$ steps, we obtain the orientation $\xi_{j+1} = (-1)^{j+1} \cdot e' \wedge e_1 \wedge \dots \wedge e_j \wedge e_0 \wedge \xi_R$ which applies to the diagram $S_{\max} = (D/e')_{\min}$, as depicted on the right of Figure 22 with positive edge e_0 so that the orientation induced from ω_{D/e_0} is now $\omega_R \wedge e_0$. With this, we calculate $\omega(S, D/e_0) = (\omega_R \wedge e_0) \rfloor \xi_{j+1} = \omega_R \rfloor (e' \wedge e_1 \wedge \dots \wedge e_j \wedge \xi_R)$.

On the other hand, we see from Remark A.8, that $\xi_{(D/e')_{\min}} = (-1)^{j+1} \cdot e' \wedge e_1 \wedge \dots \wedge e_j \wedge e_0 \wedge \xi_R$. Since $\omega_{D/e'} = \omega_R \wedge e_0$, we obtain $\omega(S, D/e') = (\omega_R \wedge e_0) \rfloor \xi_{(D/e')_{\min}} = \omega_R \rfloor (e' \wedge e_1 \wedge \dots \wedge e_j \wedge \xi_R)$, which coincides with $\omega(S, D/e_0)$.

The cases where $S_{\max} < (D/e')_{\min}$ apply the same local moves and change the signs in $p(D/e_0, \dots)$ and $p(D/e', \dots)$ the same way, establishing equality of $\omega(S, D/e_0) = \omega(S, D/e')$.

This completes the sign check for Case 2, and with this the proof of the lemma. \square

Lemma D.2. Let $(B, f_\cup, m, \omega_B^{\text{std}}) \in Q_n \hat{\mathcal{A}}$ be a maximal binary diagram, i.e. one of the following three diagrams,



On the other hand,

$$p \left(\sum_j (-1)^{j+1} \left(\text{diagram} \right) \omega_j \right) = \sum_r T_n^{r,0},$$

with the sign calculated as follows: Denote by B' and B'' the subtrees of B_{e_j} such that $B_{e_j} = B' \circ_{e_j} B''$. Then $\omega_{B'}^{\text{std}} = e_1 \wedge \cdots \wedge e_{j-1}$ and $\omega_{B''}^{\text{std}} = e_{j+1} \wedge \cdots \wedge e_{n-2}$ so that

$$(B_{e_j}, f_{\circlearrowleft}, m_{e_j}, \omega_j) = (B', f_{\circlearrowleft}, m, \omega_{B'}^{\text{std}}) \circ_{j+1} (B'', f_{\circlearrowleft}, m, \omega_{B''}^{\text{std}})$$

Thus

$$\begin{aligned} (-1)^{j+1} p(B_{e_j}, f_{\circlearrowleft}, m_{e_j}, \omega_j) &= (-1)^{j+1} p(B', f_{\circlearrowleft}, m, \omega_{B'}^{\text{std}}) \circ_{j+1} p(B'', f_{\circlearrowleft}, m, \omega_{B''}^{\text{std}}) \\ &= (-1)^{j+1} (c', f_{\circlearrowleft}, +1) \circ_{j+1} (c'', f_{\circlearrowleft}, +1) \\ &= (-1)^{j+1+(j+1)(n-j+1)+(j+1)(n-2-j)} \\ &\quad \cdot (c' \circ_{e_j} c'', f_{\circlearrowleft}, +e_j) \\ &= (c' \circ_{e_j} c'', f_{\circlearrowleft}, +e_j). \end{aligned}$$

Next, we consider the case $B = (M_{k,l})_{\max}$. We will show that the following diagram commutes:

$$\begin{array}{ccc} \begin{array}{c} \text{diagram} \\ \downarrow \partial_Q \\ \partial_Q((M_{k,l})_{\max}) \end{array} & \xrightarrow{p} & \begin{array}{c} \text{diagram} \\ \downarrow \partial_C \\ \sum_{r,s} M_{k,l}^{r,s} + \sum_{r,s} N_{k,l}^{r,s} + \sum_{r,s} O_{k,l}^{r,s} \end{array} \end{array}$$

where $\omega_{(M_{k,l})_{\max}}^{\text{std}} = (-1)^k \cdot e_1 \wedge \cdots \wedge e_{k+l-1}$; and the module trees

$$\begin{aligned} M_{k,l}^{r,s} &= \begin{array}{c} \text{diagram} \end{array} \\ N_{k,l}^{r,s} &= \begin{array}{c} \text{diagram} \end{array} & O_{k,l}^{r,s} &= \begin{array}{c} \text{diagram} \end{array} \end{aligned}$$

have orientation $+e$, where e is the unique edge in the diagram. Now:

$$\partial_Q((M_{k,l})_{\max}) = \sum_{e_j} (-1)^j \left(\begin{array}{c} \text{diagram} \\ - \text{diagram} \end{array} \right)$$

Furthermore,

$$p \left(\sum_j (-1)^j \begin{array}{c} \text{diagram with } j \text{ edges} \\ \text{trunk} \end{array} \right) = \sum_{r>0} \sum_s O_{k,l}^{r,s} + \sum_r \sum_{0<s<l} M_{k,l}^{r,s}$$

and

$$p \left(\sum_j (-1)^{j+1} \begin{array}{c} \text{diagram with } j \text{ edges and } n \text{ trunk} \\ \text{trunk} \end{array} \right) = \sum_s O_{k,l}^{0,s}.$$

Write $B_{e_j} = B' \circ_{e_j} B''$. Then $\omega_{B'}^{\text{std}} = (-1)^k \cdot e_1 \wedge \cdots \wedge e_{j-1}$, and $\omega_{B''}^{\text{std}} = e_{j+1} \wedge \cdots \wedge e_{k+l-1}$, so that

$$(B_{e_j}, f_{\circlearrowleft}, m_{e_j}, \omega_j) = (B', f_{\circlearrowleft}, m, \omega_{B'}^{\text{std}}) \circ_{j+1} (B'', f_{\circlearrowleft}, m, \omega_{B''}^{\text{std}}).$$

Thus

$$\begin{aligned} (-1)^{j+1} p(B_{e_j}, f_{\circlearrowleft}, m_{e_j}, \omega_j) &= (-1)^{j+1} p(B', f_{\circlearrowleft}, m, \omega_{B'}^{\text{std}}) \circ_{j+1} p(B'', f_{\circlearrowleft}, m, \omega_{B''}^{\text{std}}) \\ &= (-1)^{j+1} (c', f_{\circlearrowleft}, +1) \circ_{j+1} (c'', f_{\circlearrowleft}, +1) \\ &= (-1)^{j+1+(j+1)(k+l+1-j+1)+(j+1)(k+l-1-j)} \\ &\quad \cdot (c' \circ_{e_j} c'', f_{\circlearrowleft}, +e_j) \\ &= (c' \circ_{e_j} c'', f_{\circlearrowleft}, +e_j). \end{aligned}$$

Finally, we consider $B = (I_{k,l})_{\text{max}}$. We will show the following diagram commutes:

$$\begin{array}{ccc} \begin{array}{c} \text{diagram with } e_{k+l} \dots e_{k+1} \text{ and } e_1 \dots e_k \\ \text{trunk} \end{array} & \xrightarrow{p} & \begin{array}{c} \text{diagram with } l \text{ edges} \\ \text{trunk} \end{array} \\ \downarrow \partial_Q & & \downarrow \partial_C \\ \partial_Q((I_{k,l})_{\text{max}}) & \xrightarrow{p} & \sum_{r,s} I_{k,l}^{r,s} + \sum_{r,s} J_{k,l}^{r,s} + \sum_{r,s} K_{k,l}^{r,s} + \sum_{r,s} L_{k,l}^{r,s} \end{array}$$

where $\omega_{(I_{k,l})_{\text{max}}}^{\text{std}} = (-1)^l \cdot e_1 \wedge \cdots \wedge e_{k+l}$ was calculated in Example A.7, and

$$\begin{aligned} I_{k,l}^{r,s} &= \begin{array}{c} \text{diagram with } r \text{ edges on left, } s \text{ on right} \\ \text{trunk} \end{array} & J_{k,l}^{r,s} &= \begin{array}{c} \text{diagram with } s \text{ edges on left, } r \text{ on right} \\ \text{trunk} \end{array} \\ K_{k,l}^{r,s} &= \begin{array}{c} \text{diagram with } r \text{ edges on top, } s \text{ on bottom} \\ \text{trunk} \end{array} & L_{k,l}^{r,s} &= \begin{array}{c} \text{diagram with } s \text{ edges on top, } r \text{ on bottom} \\ \text{trunk} \end{array} \end{aligned}$$

have orientation $+e$, with e being the unique edge in the diagram. Now, $\partial_Q((I_{k,l})_{\text{max}})$ equals

$$\begin{aligned}
 &= (-1) \text{diagram} - (-1) \text{diagram} + \sum_{e_j} (-1)^j \left(\text{diagram} - \text{diagram} \right) \\
 &+ (-1)^{k+1} \text{diagram} - (-1)^{k+1} \text{diagram} + \sum_{e_j} (-1)^j \left(\text{diagram} - \text{diagram} \right).
 \end{aligned}$$

Again, all of these terms have orientation $\omega_j = (-1)^l \cdot e_1 \wedge \cdots \wedge \widehat{e}_j \wedge \cdots \wedge e_{k+l-1}$. We evaluate p as follows. First,

$$p \left((-1) \text{diagram} \right) = \sum_s I_{k,l}^{1,s}$$

and

$$p \left(\text{diagram} \right) = J_{k,l}^{k,0}.$$

Writing $B_{e_1} = B' \circ_{e_1} B''$ gives $\omega_{B'}^{\text{std}} = (-1)^l \cdot e_{k+1} \wedge \cdots \wedge e_{k+l}$ and $\omega_{B''}^{\text{std}} = e_2 \wedge \cdots \wedge e_k$. This gives

$$\begin{aligned}
 (B_{e_1}, f_\circ, m_{e_1}, \omega_1) &= (-1)^{l(k-1)} (B', f_\circ, m, \omega_{B'}^{\text{std}}) \circ_2 (B'', f_\circ, m, \omega_{B''}^{\text{std}}). \\
 \text{Thus } p(B_{e_1}, f_\circ, m_{e_1}, \omega_1) &= (-1)^{l(k-1)} p(B', f_\circ, m, \omega_{B'}^{\text{std}}) \circ_2 p(B'', f_\circ, m, \omega_{B''}^{\text{std}}) \\
 &= (-1)^{l(k-1)} (c', f_\circ, +1) \circ_2 (c'', f_\circ, +1) \\
 &= (-1)^{l(k-1)+2(k+1+1)+l(k+1)} (c' \circ_{e_1} c'', f_\circ, +e_1) \\
 &= (c' \circ_{e_1} c'', f_\circ, +e_1).
 \end{aligned}$$

Second,

$$p \left(\sum_j (-1)^j \text{diagram} \right) = \sum_{r \geq 2} \sum_s I_{k,l}^{r,s} + \sum_r \sum_s K_{k,l}^{r,s}$$

and

$$p \left(\sum_j (-1)^{j+1} \text{diagram} \right) = \sum_{r < k} J_{k,l}^{r,0}.$$

Writing $B_{e_j} = B' \circ_{e_j} B''$ gives $\omega_{B'}^{\text{std}} = (-1)^l \cdot e_1 \wedge \cdots \wedge e_{j-1} \wedge e_{k+1} \wedge \cdots \wedge e_{k+l}$, and $\omega_{B''}^{\text{std}} = e_{j+1} \wedge \cdots \wedge e_k$. This gives,

$$(B_{e_j}, f_\circ, m_{e_j}, \omega_j) = (-1)^{l(k-j)} (B', f_\circ, m, \omega_{B'}^{\text{std}}) \circ_{j+1} (B'', f_\circ, m, \omega_{B''}^{\text{std}})$$

Thus

$$\begin{aligned}
 (-1)^{j+1} p(B_{e_j}, f_\circ, m_{e_j}, \omega_j) &= (-1)^{j+1+l(k+j)} \\
 &\quad \cdot p(B', f_\circ, m, \omega_{B'}^{\text{std}}) \circ_{j+1} p(B'', f_\circ, m, \omega_{B''}^{\text{std}}) \\
 &= (-1)^{j+1+l(k+j)} (c', f_\circ, +1) \circ_{j+1} (c'', f_\circ, +1) \\
 &= (-1)^{j+1+l(k+j)+(j+1)(k-j+2+1)+(l+j+1)(k-j)} \\
 &\quad \cdot (c' \circ_{e_j} c'', f_\circ, +e_j)
 \end{aligned}$$

$$= (c' \circ_{e_j} c'', f_{\circ}, +e_j).$$

Third,

$$p \left((-1)^{k+1} \begin{array}{c} \text{////} \\ \text{---} \bullet \text{---} \\ \text{////} \end{array} \right) = \sum_r J_{k,l}^{r,1}$$

and

$$p \left((-1)^k \begin{array}{c} \text{////} \\ \text{---} \overset{n}{\square} \bullet \text{---} \\ \text{////} \end{array} \right) = I_{k,l}^{0,l}.$$

Writing $B_{e_{k+1}} = \sigma \cdot (B' \circ_{e_{k+1}} B'')$ gives $\omega_{B'}^{\text{std}} = e_1 \wedge \cdots \wedge e_k$, and $\omega_{B''}^{\text{std}} = e_{k+2} \wedge \cdots \wedge e_{k+l}$, where $\sigma \in S_{k+l+2}$ is the cyclic permutation “ $+(l+1) \pmod{k+l+2}$ ”. This gives,

$$(B_{e_{k+1}}, f_{\circ}, m_{e_{k+1}}, \omega_j) = (-1)^l \cdot \sigma \cdot ((B', f_{\circ}, m, \omega_{B'}^{\text{std}}) \circ_1 (B'', f_{\circ}, m, \omega_{B''}^{\text{std}})).$$

Thus

$$\begin{aligned} (-1)^k p(B_{e_{k+1}}, f_{\circ}, m_{e_{k+1}}, \omega_j) &= (-1)^{k+l} \\ &\quad \cdot \sigma \cdot (p(B', f_{\circ}, m, \omega_{B'}^{\text{std}}) \circ_1 p(B'', f_{\circ}, m, \omega_{B''}^{\text{std}})) \\ &= (-1)^{k+l} \sigma \cdot ((c', f_{\circ}, +1) \circ_1 (c'', f_{\circ}, +1)) \\ &= (-1)^{k+l+1(l+1+1)+(k+2)(l-1)} \\ &\quad \cdot \sigma \cdot (c' \circ_{e_{k+1}} c'', f_{\circ} \circ \sigma^{-1}, +e_{k+1}) \\ &= (c' \circ_{e_{k+1}} c'', f_{\circ}, +e_{k+1}). \end{aligned}$$

Fourth,

$$p \left(\sum_j (-1)^j \begin{array}{c} \text{////} \\ \text{---} \bullet \text{---} \\ \text{////} \end{array} \right) = \sum_r \sum_{s \geq 2} J_{k,l}^{r,s} + \sum_r \sum_s L_{k,l}^{r,s}$$

and

$$p \left(\sum_j (-1)^{j+1} \begin{array}{c} \text{////} \\ \text{---} \overset{n}{\square} \bullet \text{---} \\ \text{////} \end{array} \right) = \sum_{s < l} I_{k,l}^{0,s}.$$

Writing $B_{e_j} = \sigma \cdot (B' \circ_{e_j} B'')$ gives $\omega_{B'}^{\text{std}} = (-1)^{j-k-1} \cdot e_1 \wedge \cdots \wedge e_{j-1}$, and $\omega_{B''}^{\text{std}} = e_{j+1} \wedge \cdots \wedge e_{k+l}$, where $\sigma \in S_{k+l+2}$ is the cyclic permutation “ $+(k+l+1-j) \pmod{k+l+2}$ ”. This gives,

$$(B_{e_j}, f_{\circ}, m_{e_j}, \omega_j) = (-1)^{l+j-k-1} \sigma \cdot ((B', f_{\circ}, m, \omega_{B'}^{\text{std}}) \circ_1 (B'', f_{\circ}, m, \omega_{B''}^{\text{std}})).$$

Thus

$$\begin{aligned} (-1)^{j+1} p(B_{e_j}, f_{\circ}, m_{e_j}, \omega_j) &= (-1)^{k+l} \\ &\quad \cdot \sigma \cdot (p(B', f_{\circ}, m, \omega_{B'}^{\text{std}}) \circ_1 p(B'', f_{\circ}, m, \omega_{B''}^{\text{std}})) \\ &= (-1)^{k+l} \sigma \cdot ((c', f_{\circ}, +1) \circ_1 (c'', f_{\circ}, +1)) \\ &= (-1)^{k+l+1 \cdot (k+l-j+2+1) + (j+1)(k+l-j)} \\ &\quad \cdot \sigma \cdot (c' \circ_{e_j} c'', f_{\circ} \cdot \sigma^{-1}, +e_j) \\ &= (-1)^{(j+1)(k+l-j+1)} \sigma \cdot (c' \circ_{e_j} c'', f_{\circ} \cdot \sigma^{-1}, +e_j) \\ &= (c' \circ_{e_j} c'', f_{\circ}, +e_j). \end{aligned}$$

This completes the proof the lemma. □

REFERENCES

- BV. J.M. Boardman, R.M. Vogt, *Homotopy invariant algebraic structures on topological spaces*, Springer LNM 347, 1973
- C. C.-H. Cho, *Strong homotopy inner product of an A-infinity algebra*, Int. Math. Res. Not., no. 41, 2008
- L. J.-L. Loday, *The diagonal of the Stasheff polytope*, preprint arXiv:0710.0572v2
- LT. R. Longoni, T. Tradler, *Homotopy Inner Products for Cyclic Operads*, Journal of Homotopy and Related Structures, vol. 3(1), 2008, pp. 343-358, 2008
- MacL. S. Mac Lane, *Categories for the Working Mathematician*, Springer, Graduate Texts in Mathematics 5, 1971
- MS. M. Markl, S. Shnider, *Associahedra, cellular W-construction and products of A_∞ algebras*, Trans. of the AMS, Vol. 358, No. 6, pp. 2353-2372, 2005
- SU. S. Sanedlidze, R. Umble, *Diagonals on the Permutahedra, Multiplihedra and Associahedra*, Homology, Homotopy and Applications, vol.6(1), pp.363–411, 2004
- S. J. Stasheff, *Homotopy Associativity of H-Spaces. I*, Trans. AMS, Vol. 108, No. 2, pp. 275-292, 1963
- Ta. D. Tamari, *The algebra of bracketings and their enumeration*, Nieuw Arch. Wisk. (3) 10, 1962, pp. 131–146.
- TT. J. Terilla, T. Tradler, *Deformations of associative algebras with inner products*, Homology, Homotopy, and Applications 8(2), p. 115-131, 2006
- T1. T. Tradler, *Infinity Inner Products on A-Infinity Algebras*, Journal of Homotopy and Related Structures, vol. 3(1), pp. 245-271, 2008
- T2. T. Tradler, *The BV Algebra on Hochschild Cohomology Induced by Infinity Inner Products*, Annales de L'institut Fourier, vol. 58, no. 7, p. 2351-2379, 2008
- TZ. T. Tradler, M. Zeinalian, *Algebraic String Operations*, K-Theory, vol. 38, no. 1, 2007

THOMAS TRADLER, DEPARTMENT OF MATHEMATICS, COLLEGE OF TECHNOLOGY, CITY UNIVERSITY OF NEW YORK, 300 JAY STREET, BROOKLYN, NY 11201, USA
E-mail address: ttradler@citytech.cuny.edu

DEPARTMENT OF MATHEMATICS, MILLERSVILLE UNIVERSITY OF PENNSYLVANIA, MILLERSVILLE, PA. 17551
E-mail address: ron.umble@millersville.edu